DIRECT SPECTROSCOPY IN HOLLOW OPTICAL WITH FIBER-BASED OPTICAL FREQUENCY COMBS

Kristan Corwin
KANSAS STATE UNIVERSITY

07/09/2015
Final Report

REPORT DOCUMENTATION PAGE

Form Approved
OMB No. 0704-0188

The public reporting burden for this collection of information is estimated to average 1 hour per response, including the time for reviewing instructions, searching existing data sources, gathering and maintaining the data needed, and completing and reviewing the collection of information. Send comments regarding this burden estimate or any other aspect of this collection of information, including suggestions for reducing the burden, to Department of Defense, Executive Services, Directorate (0704-0188). Respondents should be aware that notwithstanding any other provision of law, no person shall be subject to any penalty for failing to comply with a collection of information if it does not display a currently valid OMB control number.
PLEASE DO NOT RETURN YOUR FORM TO THE ABOVE ORGANIZATION.

1. REPORT DATE *(DD-MM-YYYY)* 20-07-2015	2. REPORT TYPE Final Performance	3. DATES COVERED *(From - To)* 01-06-2011 to 31-05-2015

4. TITLE AND SUBTITLE
DIRECT SPECTROSCOPY IN HOLLOW OPTICAL WITH FIBER-BASED OPTICAL FREQUENCY COMBS

5a. CONTRACT NUMBER

5b. GRANT NUMBER
FA9550-11-1-0096

5c. PROGRAM ELEMENT NUMBER

6. AUTHOR(S)
Kristan Corwin

5d. PROJECT NUMBER

5e. TASK NUMBER

5f. WORK UNIT NUMBER

7. PERFORMING ORGANIZATION NAME(S) AND ADDRESS(ES)
KANSAS STATE UNIVERSITY
2 FAIRCHILD HALL
MANHATTAN, KS 665061100 US

8. PERFORMING ORGANIZATION REPORT NUMBER

9. SPONSORING/MONITORING AGENCY NAME(S) AND ADDRESS(ES)
AF Office of Scientific Research
875 N. Randolph St. Room 3112
Arlington, VA 22203

10. SPONSOR/MONITOR'S ACRONYM(S)
AFOSR

11. SPONSOR/MONITOR'S REPORT NUMBER(S)

12. DISTRIBUTION/AVAILABILITY STATEMENT
A DISTRIBUTION UNLIMITED: PB Public Release

13. SUPPLEMENTARY NOTES

14. ABSTRACT
Toward the creation of robust, portable frequency references in the near IR, we have isolated a single tooth from a fiber laser-based optical frequency comb for nonlinear spectroscopy and thereby directly referenced the comb. An 89 MHz erbium fiber laser frequency comb is directly stabilized to the P(23) (1539.43 nm) overtone transition of $12C2H2$ inside a hollow-core photonic crystal fiber. To do this, a single comb tooth is isolated and amplified from 20 nW to 40 mW with sufficient fidelity to perform saturated absorption spectroscopy. The fractional stability of the comb, ~ 7 nm away from the stabilized tooth, is shown to be 610-12 at 100 ms gate time, which is over an order of magnitude better than that of a comb referenced to a GPS-disciplined Rb oscillator.

15. SUBJECT TERMS
spectroscopy, frequency combs, hollow optical fibers

16. SECURITY CLASSIFICATION OF:			17. LIMITATION OF ABSTRACT	18. NUMBER OF PAGES	19a. NAME OF RESPONSIBLE PERSON
a. REPORT	b. ABSTRACT	c. THIS PAGE			Kristan Corwin
U	U	U	UU		19b. TELEPHONE NUMBER *(Include area code)* 785-532-1663

Standard Form 298 (Rev. 8/98)
Prescribed by ANSI Std. Z39.18

Final Technical Report

PI: **Dr. Kristan L. Corwin**
Institution: **Kansas State University**
Address: **Department of Physics**
                       116 Cardwell Hall
                       Manhattan, KS 66506
Phone: **(785) 532-1663**
E-mail: **corwin@phys.ksu.edu**

Abstract:
Toward the creation of robust, portable frequency references in the near IR, we have isolated a single tooth from a fiber laser-based optical frequency comb for nonlinear spectroscopy and thereby directly referenced the comb. An 89 MHz erbium fiber laser frequency comb is directly stabilized to the P(23) (1539.43 nm) overtone transition of $^{12}C_2H_2$ inside a hollow-core photonic crystal fiber. To do this, a single comb tooth is isolated and amplified from 20 nW to 40 mW with sufficient fidelity to perform saturated absorption spectroscopy. The fractional stability of the comb, ~ 7 nm away from the stabilized tooth, is shown to be 6×10^{-12} at 100 ms gate time, which is over an order of magnitude better than that of a comb referenced to a GPS-disciplined Rb oscillator.

Furthermore, gas-filled hollow optical fiber references based on the P(13) transition of the $v_1 + v_3$ band of $^{12}C_2H_2$ promise portability with moderate accuracy and stability. Previous realizations are corrected ($< 1\sigma$) using proper modeling of a shift due to line-shape. To improve portability, a sealed photonic microcell (PMC) is characterized on the $^{12}C_2H_2$ $v_1 + v_3$ P(23) transition with somewhat reduced accuracy and stability. Effects of the photonic crystal fiber, including surface modes, are explored. Both polarization-maintaining (PM) and non-PM 7-cell photonic bandgap fiber are shown to be unsuitable for kHz level frequency references.

Toward improving the portability of the system, Perturbed Resonance for Improved Single Modedness (PRISM) fiber is employed for saturated absorption spectroscopy in a molecular gas. Reduced alignment sensitivity, lack of surface modes, and ease of angle splicing make it promising for portable gas-filled frequency references.

DIRECT SPECTROSCOPY IN HOLLOW OPTICAL FIBER WITH FIBER-BASED OPTICAL FREQUENCY COMBS

Overview

This document represents the culmination of a decade worth of work in gas-filled hollow optical fibers toward the development of portable optical frequency references. However, only the accomplishments since the last final report, in late 2010, are detailed here. All of the results under discussion have been published, with the exception of an active invention disclosure. Therefore, the results below are drawn from our published work.

One aspect of this work involved the demonstration of improved hollow fiber optical frequency references toward a robust and portable reference, useful for example as a short-term alternative to GPS. Another involved the demonstration of efficient ways of locking an optical frequency comb to a gas-filled fiber reference without the intermediate stable cw laser, toward compact and efficient implementations of stabilized near-IR optical frequency combs. Both are described in detail below.

I. Direct fiber comb stabilization to a gas-filled hollow-core photonic crystal fiber
This material was previously published in Ref. [1] and in Ref.'s [2], [3], and [4].

Optically referenced combs demonstrate superior short-term instability [5] limited by that of the optical reference. Typically, optically referenced frequency combs require a stable cw laser locked to an optical cavity and/or an atomic or molecular reference. However, direct comb spectroscopy eliminates the need for a cw laser, which is advantageous for portable, practical systems, for which fiber-laser-based combs are well-suited [6, 7]. Hu *et al.* [8] have directly optically referenced an Er fiber laser-based frequency comb to a Rb cell by generating its second harmonic and stabilizing to the two-photon transition in Rb. Heinecke *et al.* [9] have demonstrated an optically-referenced Ti:sapphire comb by stabilizing a single tooth to a Rb transition using saturated absorption spectroscopy (SAS). However, application of this technique to a low repetition rate fiber frequency comb in the near IR offers unique challenges. In particular, sufficient power per tooth of the comb must be obtained, either by increasing the repetition rate of the laser or by amplifying the frequency comb, or both.

Fiber lasers with repetition rates of 1-10 GHz have been created [10-14], but are difficult to fully stabilize. In 2012, Chao *et al.* for the first time successfully phase stabilized a ~ 1 GHz erbium fiber laser [15] based on a linear cavity. However, this laser required extreme amplification to generate supercontinuum (SC) for self-referencing. Delfyett's group [12, 13] built a 10 GHz harmonically mode-locked fiber laser with a Fabry-Perot etalon integrated in the laser cavity, and measured its carrier-envelope offset frequency, f_0. But the harmonic mode-locking mechanism may limit the instability, and the laser has insufficient power for f_0 generation. Injection locking of a mode-locked fiber laser has allowed creation of a fiber laser-based frequency comb with up to 1 GHz repetition rate with ~ 5.5 nm spectral bandwidth [16]. And recent advances in microresonator-based combs make them a promising option for the future [17].

An alternative way to increase the repetition rate is to use an external filtering cavity. High repetition rate, broad bandwidth fiber combs are generated in this way for astronomical calibration purposes [18, 19]. In such configurations, one of the major challenges is to optically amplify the comb without degrading the comb signal-to-noise ratio (SNR).

Our approach to single-tooth amplification builds on earlier work. Cruz *et al.* have shown an optical amplification of supercontinuum by a factor of 17 dB using a home-made semiconductor amplifier [20]. Moon *et al.* performed spectroscopy in Rb vapor by injection locking a cw laser to a phase stabilized single comb tooth [21]. In the early 1990s, the telecom industry spurred amplification of small cw light power with high gain and low noise figure [22, 23] by employing multiple small gain amplification stages to achieve high gain while preserving the SNR.

Here, as discussed in Section 2, we optically amplify a single comb tooth from 20 nW to 40 mW (by a factor of 2×10^6) while preserving the comb's SNR using multiple filtering and amplification stages.

During this process, an external filtering cavity is built to increase the pulse repetition rate from 89 MHz to 9.4 GHz. A distributed-feedback (DFB) laser is injection-locked to a 50 µW single tooth out from the filtering cavity. No shift of the comb frequency is detected at the 10 kHz level during amplification. In Section 3, the amplified single tooth is then frequency-stabilized to the P (23) v_1+v_3 overtone transition of $^{12}C_2H_2$ at ~1539.43 nm through sub-Doppler spectroscopy inside a gas-filled hollow-core photonic crystal fiber [24, 25]. With f_0 stabilized to an RF reference simultaneously, a fully phase stabilized, optically-referenced erbium fiber laser frequency comb is demonstrated. In Section 4, the comb stability is characterized through comparison with a cw laser locked to a gas-filled hollow fiber reference [25]. Section 5 outlines various ways the comb could be stabilized to the optical reference, and the resulting stability expected across the comb optical spectrum.

We believe this to be the first demonstration of an optically referenced comb based on a fiber laser using direct-comb saturated absorption spectroscopy. Furthermore, this work represents the first isolation and amplification of a single tooth directly from a sub-100 MHz fiber laser for saturated absorption spectroscopy. This comb amplification technique opens many possibilities for direct comb spectroscopy using low power, low repetition rate (< 100 MHz) fiber laser frequency combs. In addition, the fiber comb optically referenced to a gas-filled fiber reference represents a large step towards an all-fiber portable frequency metrology system with low short-term instability, independent of the global positioning system (GPS).

2. Comb tooth amplification for sub-Doppler spectroscopy

The overview setup for this work is shown in Fig. 1. Section 2.1 presents the 89 MHz fiber ring laser built for sub-Doppler spectroscopy. The majority (90%) of power from the fiber ring laser output goes for f_0 detection and stabilization at ~ 30 MHz via diode laser pump current, based on a collinear f-$2f$ interferometer [26]. The rest of the output is used for single comb tooth amplification, including multiple filtering and amplification stages (middle dashed box in Fig.1), which are discussed in Section 2.2-2.4. A small tap from the ring oscillator is used for monitoring the comb's repetition rate.
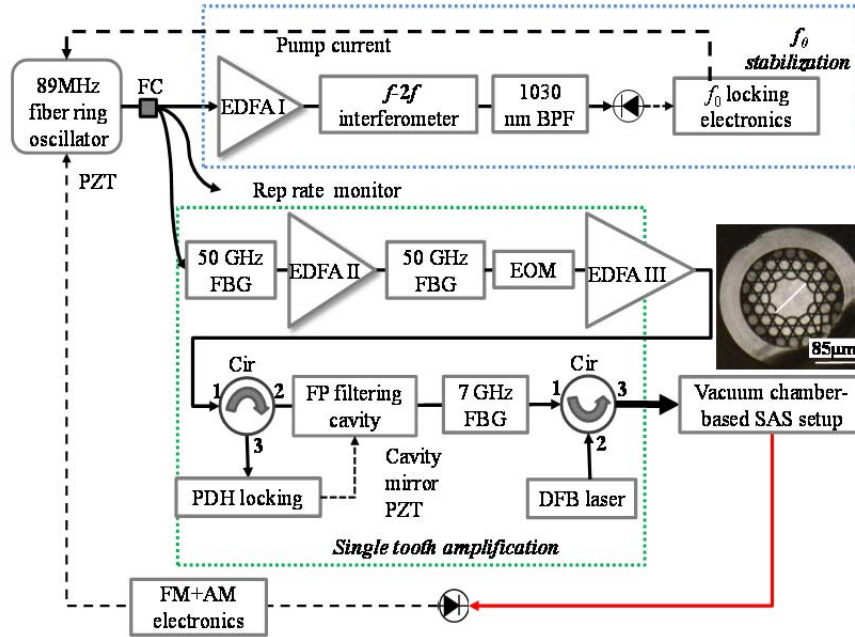

Fig. 1. Overview schematic of single tooth saturated absorption spectroscopy. FC: fiber coupler, EDFA: Er-doped fiber amplifier, BPF: band pass filter, FBG: fiber Bragg grating, EOM: electro-optic modulator, Cir: circulator, PDH: Pound-Drever-Hall, FP: Fabry-Perot, AOM: acousto-optic modulator, and AM: amplitude modulator. Solid lines indicate optical paths, and dashed lines indicate electrical paths.

2.1 The fiber ring laser

The schematic setup of the all-fiber ring laser is shown in Fig. 2 (left). The 89 MHz erbium-doped fiber ring oscillator is mode-locked using the nonlinear polarization rotation technique [27]. The gain fiber is a 64 cm erbium-doped fiber (Liekki Er110), with an absorption coefficient of 110 dB/nm at 1530 nm, pumped by a 300 mW diode laser at 980 nm. All other fibers in the cavity are standard single-mode fiber (SMF). The laser is mode-locked in the stretched pulse regime. The output spectrum has a 3-dB bandwidth of 30 nm (Fig.2 right), with a total output power of 3.8 mW.
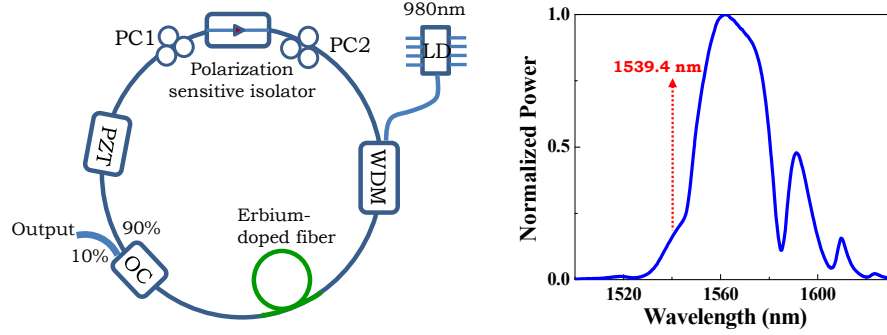

Fig. 2. Schematic setup and optical spectrum of an 89 MHz erbium-doped fiber ring laser for single tooth saturation spectroscopy. The red arrow in the spectrum indicates the wavelength of the single comb tooth to be amplified.

2.2 Comb amplification

Our initial study of comb amplification is done at 1532.83 nm. The output from the oscillator is first filtered by a 50 GHz fiber Bragg grating (FBG) and amplified by a home-made erbium fiber amplifier (EDFA II in Fig. 1), then filtered again at the same wavelength before entering a commercial polarization maintaining cw erbium-doped fiber amplifier (EDFA III in Fig. 1). The purpose of EDFA II is to generate enough light at the target wavelength to seed the following EDFA III. This EDFA II proves to be the key to preserving the comb SNR.
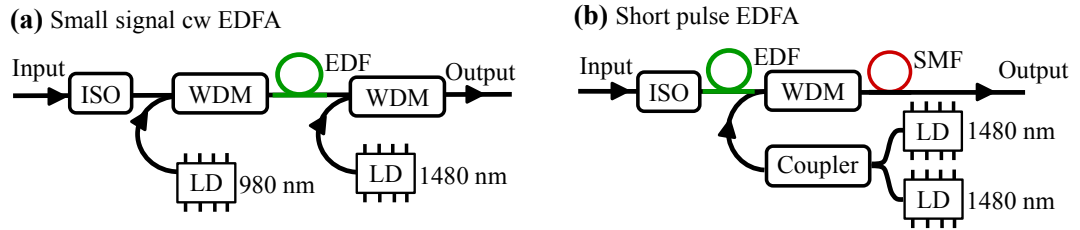

Fig. 3.Schematic setup up of (a) small signal cw EDFA, and (b) short pulse EDFA.

Figure 3(a) shows the schematic of EDFA II, which is a small signal cw EDFA [22, 23]. A 1 m length of EDF (EDF 80) with an absorption coefficient of 80 dB at 1530 nm is used as the gain fiber. The key point to this design is that a narrow bandwidth comb (~ 50 GHz) around our wavelength of interest is filtered from the oscillator output and seeded into this amplifier. The amplifier is mainly forward-pumped by a 200 mW pump diode at 980 nm, and slightly backward pumped by a 40 mW laser diode at 1480 nm. The small signal EDFA has 38 dB gain at 1532.83 nm when seeded with 1 µW cw light, and 14 dB gain when seeded with 1 mW cw light.

We initially built a short pulse EDFA, shown in Fig. 3(b), which was not successful. The main reason is that it introduced devastating amplified spontaneous emission (ASE) noise that destroyed the comb's SNR. It was designed to be seeded directly by the oscillator comb, and to broaden the comb spectrum to

have enough light at the target wavelength. The gain fiber is highly backward pumped with a total pump power of 1 W. The amplified pulses are further temporally compressed by the following SMF fiber via solitonic effects.

To characterize the comb's SNR before and after amplification, a heterodyne beat between the comb and a cw fiber laser with a much narrower linewidth (< 1 kHz) is analyzed by an electrical spectrum analyzer (HP 8561B), shown in Fig. 4. Before amplification, the beatnote has a SNR of 20 dB (mostly limited by comb power) at 1 MHz resolution bandwidth (RBW). Using the same amount of optical power for both the comb and cw laser, this SNR is well preserved after amplification by the small signal cw EDFA. However, when the short pulse EDFA is used instead, the SNR is dramatically reduced to 8 dB.

To further study how the two EDFAs behave in terms of noise and signal amplification, we measured the electronic noise floor and the SNR of the cw/comb beatnote in three scenarios, shown in Fig. 4(d). The cw fiber laser power was kept the same for all beat measurements, while the comb power was controlled by variable attenuation. The noise floor behaves like technical noise on the amplified comb. Figure 4 indicates that the small signal EDFA produces an amplified comb with a lower noise floor and higher SNR as compared to the short pulse EDFA. The degradation in SNR after the short pulse amplifier may be due to fiber nonlinearities.

Considering that there are multiple power amplification stages based on EDFAs in our setup, and also the fact that the amplified wavelength is at the edge of the erbium-doped fiber gain spectrum, we investigated the possible frequency shift introduced by all the EDFAs when seeded with the low power comb. Specifically, we measured the heterodyne beat between the pre and post amplified cw light or comb tooth. Our results show that for a cw seeding power of 100 nW and above, no obvious frequency shift is observed within 100 Hz. For comb seeds, the upper limit on the shift is 10 kHz due to low beatnote SNR.
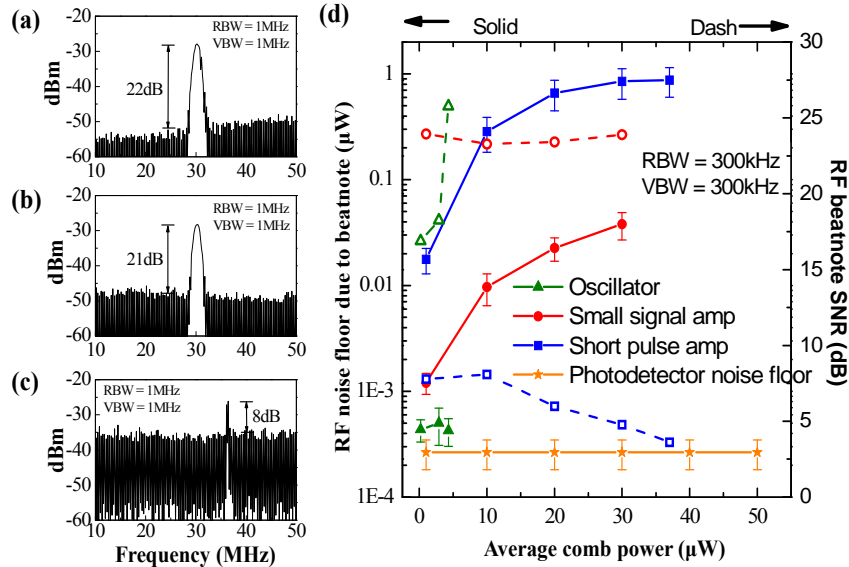

Fig. 4. RF beatnote between the cw fiber laser and (a) the oscillator comb, (b) the comb after amplification by the small signal cw EDFA, and (c) the comb after amplification by the short pulse EDFA. (d) RF noise floor for the above three beatnotes (left solid), and RF beatnote SNR (right dashed) as a function of average comb power. All measurements are taken under 300 kHz RBW.

2.3 Selection of a single tooth (filtering cavity)

A single comb tooth is selected using a free space Fabry-Perot filtering cavity followed by a narrow bandwidth fiber Bragg grating (FBG). The filtering cavity length must be adjusted such that each cavity

resonance coincides with a comb tooth frequency. Therefore, the cavity length is stabilized to multiple comb teeth simultaneously, such that the cavity free spectral range (FSR) is an integer multiple of the comb repetition rate. In our case, one comb tooth is selected out of ~ 105 teeth. Before passing through the cavity, a 50 GHz narrow bandwidth comb is amplified by a commercial cw polarization-maintaining EDFA (by Manlight, EDFA III in Fig. 1) to an average power of 200 mW.

The cavity consists of two nearly plano dielectric mirrors (with 50 cm radius of curvature) separated by 1.6 cm. One of the mirrors is attached to a ring PZT (Nolia) for cavity length stabilization. A collimated beam with 0.5 mm $1/e^2$ diameter is focused by a 200 mm lens to ensure required mode matching with the cavity mirror curvature. The cavity has a finesse of about 250, and a suppression ratio of at least 21 dB as measured by a heterodyne beatnote between the filtered comb and a cw fiber laser. When the cavity is not resonant with the laser, light reflected from the first cavity mirror will be rejected back to the third port of the fiber circulator before the cavity, used for Pound-Drever-Hall locking, which will be discussed in more detail in Section 3. The filtered 9.4 GHz comb from the cavity output is coupled back into the fiber and further spectrally filtered by a customized FBG, with 3-dB bandwidth of 7 GHz, to obtain a single comb tooth. The FBG is under precise temperature control to have a stable central transmission wavelength at ~ 1539.4 nm. The single comb tooth after the FBG has an optical average power of ~ 50 μW, which is sufficient for injection locking the DFB laser in the last amplification stage (Section 2.4).

2.4 Injection locking DFB laser

The last comb amplification step is accomplished by seeding the single comb tooth into a distributed-feedback (DFB) laser diode. This allows stable injection locking of the DFB laser output to the seeding comb tooth. The DFB laser is a customized 14-pin butterfly pump laser diode (FITEL) without built-in isolator. The key to a stable injection lock is to seed the DFB laser with only one comb tooth. This was verified by seeding the DFB laser with two identical cw fiber lasers at 1532.8 nm with equal optical power to mimic the case when two comb teeth are injected into the DFB laser. Our results show that even when the two cw lasers are a few GHz apart, the DFB laser injection locks to each of the two seeds at different times, indicating mode competition between the seeds. This determines that the FSR of the filtering cavity has to be larger than the bandwidth of the following 7 GHz FBG.

For stable injection locking, the DFB laser diode is temperature-controlled at 32.92 °C, pumped by a current of 170 mA, and amplifies the injected single tooth to be 40 mW at 1539.43 nm. Figure 5(b) shows a stable RF beatnote between the amplified single tooth using a similar DFB laser at 1532.83 nm and cw fiber laser. The beatnote SNR is enhanced to be ~40 dB at 1 MHz RBW.

2.5 Single tooth saturated absorption spectroscopy

A 40 mW comb tooth is then directed to the saturated absorption spectroscopy (SAS) setup to generate a sub-Doppler error signal, as shown in the lower (green) dashed box in Fig.1. Details of the setup can be found in [25]. Acetylene gas is loaded inside a 7.9 m length of hypocycloid shaped core-contour kagome-structured hollow-core photonic crystal fiber, with a core size of 85 μm [24, 28] and its pressure was set at 140 mtorr (18.7 Pa).

3. Frequency comb stabilization

To fully stabilize the comb, there are three servo loops, shown in Fig. 1, that lock the carrier offset frequency f_0 to an RF synthesizer referenced to a GPS-disciplined Rb oscillator (GPS-Rb), stabilize the filtering cavity to the comb for proper filtering of every one out of ~ 105 comb teeth, and frequency stabilize the amplified single comb tooth to the P(23) overtone transition of $^{12}C_2H_2$ at 1539.43 nm. The technique employed for f_0 locking is described in [26]. Here, f_0 can be locked within a few Hz for over ten hours. This section focuses on the last two servo loops. A GPS-Rb oscillator serves as the external reference for all synthesizers and frequency counters.

The filtering cavity is stabilized to a particular comb tooth using the Pound-Drever-Hall (PDH) technique [29]. Due to limited tunability of the fiber laser-based comb, this particular tooth of the 89 MHz

comb has to be chosen as close to the P(23) line as possible. To select that tooth, a cw diode laser (Santec TSL-210) is stabilized to the P(23) transition as a reference laser and beat against the filtering cavity output. The cavity length is scanned to be resonant with a number of different comb teeth, until the optical heterodyne beat is close to zero frequency. For PDH locking, the comb is modulated at 30 MHz by using an electric-optical modulator. Although the PDH error signal generated by the comb has a SNR of about 20, a factor of 6 lower than that generated by a cw fiber laser as the source because most detected comb teeth do not contribute to the error signal. However, using a homemade servo box, we are still able to lock the cavity for hours.

The error signal for locking the single tooth to the P(23) overtone transition is similar to that of a cw fiber laser, which can be found in [25]. Both sub-Doppler error signals have SNR's above 100 within 60 kHz bandwidth, shown in Fig. 6. This sub-Doppler error signal is fed back to the fiber ring laser PZT for precise control of f_{rep}.

The amplified comb tooth would be more wavelength-tunable if the injection-locked DFB laser were replaced with an EDFA. We investigated this approach using a commercial cw EDFA and observed an error signal but with much worse SNR of only 4. This SNR degradation is likely due to non-uniform power amplification of the suppressed teeth from the cavity as revealed on an RF spectrum analyzer by increased power at the 89 MHz repetition rate. Comparing with this EDFA technique, the amplification technique using injection locking is superior because the small gain bandwidth of the DFB laser and the minimum power threshold for stable locking ensure that only a single comb tooth can be amplified. In the end, the error signal shown in Fig. 5(a), generated from injection locking the DFB laser, is used to stabilize a comb tooth at 1539.43 nm to the P(23) overtone transition of acetylene. With the offset frequency f_0 locked to an RF reference and one comb tooth locked to an acetylene transition, both degrees of freedom of the comb are stabilized. The system can stay locked for tens of hours.
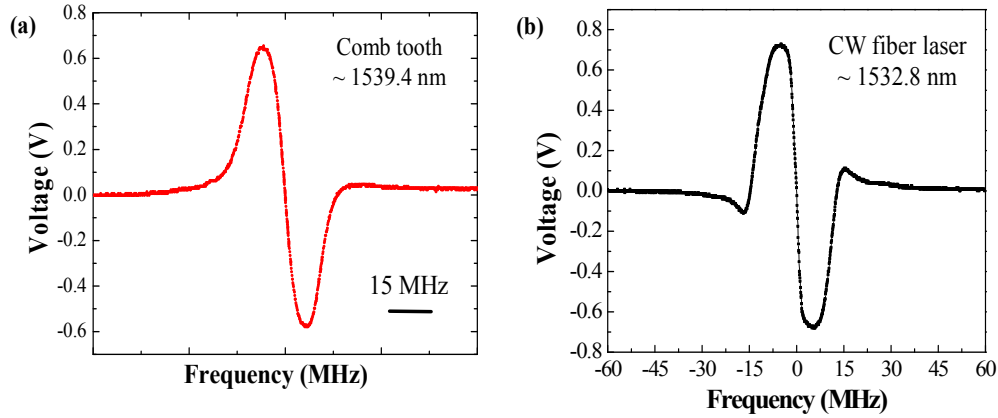

Fig. 5. The sub-Doppler error signal generated from (a) an amplified single tooth, and (b) a cw fiber laser.

4. Optical instability measurement

Once the comb is stabilized as described in Section 3, the comb stability is characterized by a comparison with a cw reference at 1532.83 nm, which is ~ 7 nm away from the stabilized single tooth, shown in Fig. 6(a). This cw reference is a cw fiber laser locked to the P (13) line of $^{12}C_2H_2$ inside gas-filled hollow-core fiber [25] using the same SAS technique as the one described for the single tooth locking. The error signal for locking is plotted in Fig. 5(a). The stabilized comb is optically combined with the cw reference, resulting in an RF beatnote.

The fractional instability (Allan deviation) of the optical tooth at 1532.83 nm is calculated from the RF beat, as show in Fig. 6(b) (red dots). Since the fluctuation of the measured RF signal is divided by the optical frequency in THz, this result is not limited by the GPS-Rb-referenced counter (black stars). It has short time stability of 6×10^{-12} at 100ms gate time, which is over an order of magnitude better than the

GPS-Rb oscillator (black stars). The stability of the cw reference used for comparison was extrapolated from two previous measurements. One is the heterodyne beating of two identical cw fiber references in our lab [30], shown in blue squares, which is independent of the GPS limit. The other is the beat between one cw fiber reference and a carbon nanotube fiber laser-based frequency comb [26] referenced to the GPS-Rb oscillator, originally published in [25]; the original data set has been reanalyzed to correct an error and shows improved stability at 1000 s (green diamonds). This improvement is important because it indicates the long-term stability of the cw fiber reference, which can also be expected from this fiber-referenced comb system.

Because the stability of the optically referenced comb is comparable to that of the cw reference at short time scales, the stability of our optical reference at 1539.43 nm has been transferred to the measured tooth at 1532.83 nm. The beatnote shows a slow drift at a time scale of a few hours, which correlates with drift in the repetition rate. This slow drift is independent of leakage of vacuum chambers, temperature or humidity, and is likely due to offsets in the locking electronics. We believe with improved servo electronics, the system is expected to have comparable long-term stability as the single cw reference data (green diamonds) in Fig. 6(b).
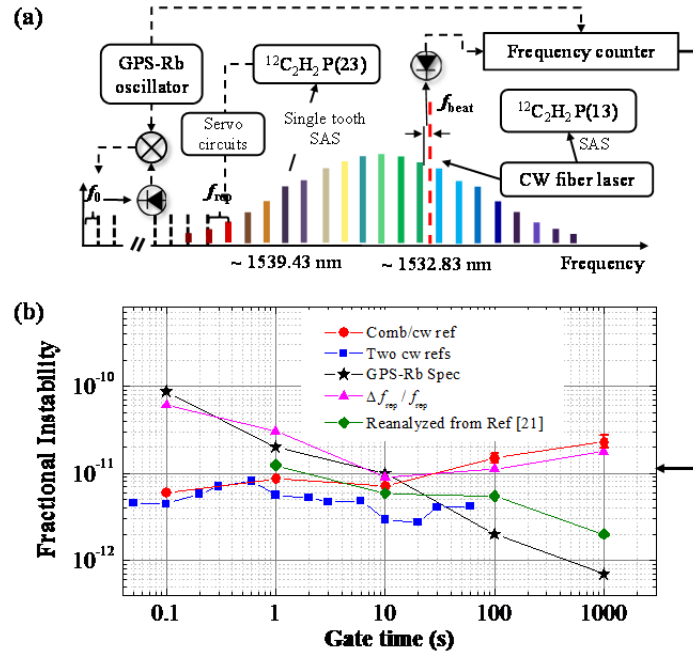

Fig. 6. (a) Schematic setup for the optically referenced comb stability measurement. (b) Fractional instabilities (Allan deviations) of: (red dots) the comb at 1532.8 nm compared to a cw fiber laser reference; (blue squares) the cw reference at 1532.8 nm extrapolated from two identical reference heterodyne beat measurement; (black stars) GPS-disciplined Rb oscillator from spec sheet; (pink triangles) comb's repetition rate frequency recorded by a GPS/Rb-referenced frequency counter; (green diamonds) reanalyzed data for Fig. 3(c) in [25]. Error bar on the red-dot line represents 1σ confidence intervals.

The instability of the RF repetition rate from the same measurement, shown in pink triangles in Fig. 6(b), is expected to follow the comb instability shown in red dots. However, the measurement is limited by the performance of the GPS-Rb oscillator at short time scales. This is because all the frequency counters used in the experiment are referenced to GPS-Rb. For a real measurement of f_{rep} stability below the GPS-Rb limit, we would have to use a better RF reference, for example, a hydrogen maser. The accuracy of this comb reference is expected to be comparable to the cw reference in [25] of ±10 kHz.

For comparison, the frequency comb of Hu *et al.* [8] is referenced to a Rb vapor cell by stabilizing a single tooth to the two-photon transition at 778 nm and f_{rep} to an electromagnetically induced transparency resonance at 3 GHz; the microwave reference limits the optical fractional instability to be about 10^{-10} at 1s, and 10^{-11} at 1000 s. Stability similar to that of Fig. 6(b) is achieved in the direct comb spectroscopy demonstrated by Heinecke *et al.* [9] based on an optically-referenced 10 GHz Ti:sapphire comb. There, a single tooth is stabilized to a Rb transition using sub-Doppler spectroscopy while the comb repetition rate is locked to a hydrogen maser. The stability of a comb tooth 20 nm away from the Rb resonance is measured to be 7×10^{-12} at 1 s gate time.

5. Comb frequency instability calculation for different locking schemes

There are many ways to stabilize a frequency comb using RF and optical references. Reference [9] describes the relative instabilities using various reference schemes. Here we specially calculate the comb stability using our gas-filled hollow-core fiber reference and RF references of various stabilities, thereby showing that good comb performance can be achieved using either the gas-filled hollow-core fiber reference with modest RF (scheme 2 below), two optical references (scheme 3), or no RF references (scheme 4). We estimate the comb stability for four different locking schemes: scheme 1, f_0 and f_{rep} locked to an RF reference; 2, f_0 locked to RF while a single comb tooth was locked to an optical reference; 3, f_{rep} locked to RF and a single comb tooth to optical reference; and 4, two comb teeth locked to two optical references. The comb instability calculations for these four locking schemes are summarized in Table 1. The degradation of the comb stability is investigated when different RF references are used, as we look 100 nm and 500 nm away from 1539.4 nm, shown in the last two columns of Table 1.

Table 1. Calculation of comb optical instability at 100 ms within 100 and 500 nm of 1539 nm when various locking schemes and RF and optical references are employed.

	Locking parameters	$\delta f_{RF}/f_{RF}$		$\delta f_{opt}/f_{opt}$	λ_{r1} (nm)	$\Delta\lambda_r{}^a$ (nm)	Comb tooth instability about 1539.4 nm	
							±100 nm	±500 nm
(1)	$f_0^{(RF)} +$ $f_{rep}^{(RF)}$	Quartz	1×10^{-9}	----	----	----	1×10^{-9}	1×10^{-9}
		GPS-Rb	2×10^{-11}				2×10^{-11}	2×10^{-11}
		H maser	1×10^{-13}				1×10^{-13}	1×10^{-13}
(2)	$f_0^{(RF)} +$ $f_{r1}^{(opt)}$	Quartz	1×10^{-9}	1×10^{-12}	1539.4	----	1×10^{-12}	1×10^{-12}
		GPS-Rb	2×10^{-11}					
		H maser	1×10^{-13}					
(3)	$f_{rep}^{(RF)} +$ $f_{r1}^{(opt)}$	Quartz	1×10^{-9}	1×10^{-12}	1539.4	----	7×10^{-11}	3×10^{-10}
		GPS-Rb	2×10^{-11}				2×10^{-12}	7×10^{-12}
		H maser	1×10^{-13}				9×10^{-13}	7×10^{-13}
(4)	$f_{r1}^{(opt)} +$ $f_{r2}^{(opt)}$	----	----	1×10^{-12}	1539.4	3 nm	7×10^{-11}	3×10^{-10}
						30 nm	5×10^{-12}	3×10^{-11}
						300 nm	2×10^{-12}	3×10^{-12}

^{a} wavelength separation between two stabilized comb teeth $\Delta\lambda_r = \lambda_{r1} - \lambda_{r2}$

In this calculation, we used the following fiber comb parameters: repetition rate is 90 MHz, f_0 is 30 MHz, and one stabilized comb tooth is at the reference wavelength $\lambda_{r1} = c/f_{r1}^{(opt)} = 1539.4$ nm (case 2-4). For the optical reference, we assume the fractional instability at 100 ms is 10^{-12}, as measured in our experiment.

In scheme 1, the instability of the mth comb tooth can be expressed as Eq. (11) of [9] in terms of the instability of f_0 and f_{rep}. The microwave instability of f_{rep} is transferred to the optical regime (ν_m) due to the large m number $\sim 10^6$ for a sub-100 MHz fiber laser. In this case, the f_0 fractional instability is essentially irrelevant. Within ± 500 nm around the stabilized comb tooth, the comb instability is dominated by the RF instability of the repetition rate.

In scheme 2, if f_0 is locked to an RF reference while one comb tooth is locked to an optical reference, the stability of the mth comb tooth can be expressed as:

$$\sigma_{\nu_m} = \frac{\delta\nu_m}{\nu_m} = \left(1 - \frac{m}{n_r}\right)\frac{\delta f_0}{\nu_m} + \frac{m}{n_r}\frac{\delta\nu_r}{\nu_m}$$

Where ν_r is the optical frequency of the stabilized comb tooth and n_r is the mode number of that tooth. In this equation, the first term is the uncertainty induced by the f_0 instability. As shown in Table 1, the f_0 instability (δf_0) is irrelevant for the resulting comb instability, and the comb instability is dominated by the second term, which depends on two parameters: the instability of the comb tooth locked to the optical reference ($\delta\nu_r$), and how far the comb tooth of interest is away from the stabilized tooth. Based to our calculation, within ± 500 nm from the stabilized comb tooth at 1539.43 nm, the uncertainty of the stabilized optical tooth is still the dominant factor.

Scheme 3 involves f_{rep} locked to an RF reference while one comb tooth is locked to an optical reference. An advantage of this locking scheme is that the generation of carrier-envelope offset frequency f_0 can be avoided, which reduces the system complexity. However, a high performance RF reference is required such that the multiplied RF instability does not dominate. The instability of the comb tooth of interest can be expressed by Eq. (5) of [9] in terms of the fractional instability of the repetition rate and the locked single tooth. This calculation shows that the optical instability depends critically on the employed RF reference.

In scheme 4, two comb teeth are stabilized to two separate optical references at wavelengths λ_{r1} and λ_{r2}, which can be two transitions from the same or different types of atoms/molecules, or high finesse optical cavities. By using gas-filled photonic microcells [30] as the optical references, the system can likely be made simpler and more portable without the integration of RF references. For simplicity, we assume that both feedback loops are identical and independent from each other. Therefore, the stability of the mth comb tooth can be expressed as:

$$\sigma_{\nu_m} = \frac{\delta\nu_m}{\nu_m} = \frac{m - n_{r2}}{n_{r1} - n_{r2}} \times \frac{\nu_{r1}}{\nu_m} \times \frac{\delta\nu_{r1}}{\nu_{r1}} + \frac{n_{r1} - m}{n_{r1} - n_{r2}} \times \frac{\nu_{r2}}{\nu_m} \times \frac{\delta\nu_{r2}}{\nu_{r2}}$$

In this case, besides the instability of the two stabilized comb teeth ($\delta\nu_{r1}/\nu_{r1}$ and $\delta\nu_{r2}/\nu_{r2}$, respectively), another key parameter that determines the overall comb instability is the wavelength separation between the two stabilized comb teeth. As an example, Table 1 shows the comb instability when two stabilized comb teeth are separated by 3 nm, 30 nm and 300 nm. If the two locked teeth are separated by only 3 nm, the comb stability degrades by almost two orders of magnitude 500 nm away from the locked tooth at 1539.4 nm. In contrast, if the separation is 300 nm, the degradation is only a factor of three even for comb teeth almost 500 nm away from one of the locked teeth. Therefore, the two stabilized comb teeth need to be at least hundreds of nanometers apart to avoid fast degradation in comb stability, which may be achievable with two separate gas-filled fiber references based on different gasses. This result is consistent with the conclusions obtained in [9].

6. Summary

We have demonstrated the first direct sub-Doppler spectroscopy with a single tooth from an optically-referenced fiber comb. To do this, a single comb tooth was amplified from 20 nW to 40 mW with high

fidelity, sufficient to perform saturated absorption spectroscopy on an overtone transition in acetylene near 1540 nm directly with the amplified comb tooth. No intermediate cw laser was required, nor did a cw laser need to be phase-locked to the comb.

The resulting optical frequency comb exhibits high short-term stability (6×10^{-12} at 100 ms) exceeding that of the GPS-disciplined Rb oscillator by an order of magnitude; thus the stability of the comb is equal to that of a cw fiber laser locked to the reference. Long-term drift is attributed to technical noise and should be readily reduced to the level of a cw laser locked to the fiber reference (shown in green diamonds in Fig. 6(b), the corrected data from [25]). Calculations indicate that f_{rep} can be read out as a source of stable RF, a factor 10 better than that of a quartz oscillator at 100 ms, when f_0 is stabilized to a modest RF reference (quartz oscillator) or a second optical reference at least 300 nm away from the first. Thus this work is a significant advance towards an all-fiber metrology system for moderate accuracy and good short-term instability in the near-IR and RF regimes without reliance on GPS.

This result demonstrates the viability of direct stabilization of a sub-100 MHz repetition rate fiber comb to a gas-filled hollow-core fiber toward an all-fiber metrology system. With some modifications, this system can be made more portable. The gas-filled hollow fiber, here mounted between two vacuum chambers, can be replaced with a sealed photonic microcell [30]. Furthermore, the 89 MHz rep rate comb with 9 GHz single stage filtering cavity may in the future be replaced with a GHz repetition rate comb based on one of many technologies [10-14, 16].

Acknowledgments

II. Acetylene Frequency References in Gas-filled Hollow Optical Fiber and Photonic Microcells
This material was previously published in Ref. [31].

1.   Introduction
High precision frequency references near 1.5 μm are desirable for optical sensing, optical telecommunications, metrology and many other applications. Using the technique of saturated absorption spectroscopy (SAS) inside a power build-up cavity [32, 33] and vapor cell [34], 1 kHz accuracy frequency references have been created. However, those acetylene frequency references are realized in free-space and cavity configurations [34, 35] that require -large containers to fulfill the required interaction lengths and high saturation intensities. The advent of gas-filled hollow-core photonic crystal fibers (HC-PCF) [36] and its sealed form, the photonic microcell (PMC) [37], enable a portable and robust alternative to traditional gas-filled glass cell-based molecular frequency standards as illustrated in several publications [25, 38-40].

   SAS inside HC-PCFs allows us to build a robust and portable frequency reference. More importantly, the fiber geometry can give long interaction lengths between the filling gas and the laser field, and the low loss of HC-PCF facilitates the optical interactions with low power levels. Although the small core size limits the linewidth of statured absorption features, fiber-based spectroscopy can still provide high accuracy frequency measurements. We previously demonstrated a 10 kHz accuracy frequency reference on a $^{12}C_2H_2$ transition inside a hollow-core fiber between two vacuum chambers [25], about two orders of magnitude better than previously reported in fiber [41].

   Here, we have improved the characterization of the short-term stability of the P(13) $v_1 + v_3$ transition in $^{12}C_2H_2$ by constructing a second vacuum chamber reference similar to that described in [25] and making a three-cornered hat measurement. In addition, a small correction (< 1σ) to the absolute frequency is calculated and applied to the previous results [25], based on careful modeling of lineshape [42], which gives better agreement with published values [43, 44]. Also further studies of the polarization sensitivity and the surface modes of the fiber-based frequency reference are made.

   Our ultimate goal is to produce portable gas-filled references that exhibit similar accuracy and stability to that seen with the gas-filled fiber vacuum chamber reference system. To that end, we have developed gas-filled PMCs [37, 45, 46] based on photonic bandgap and kagome-structured HC-PCFs. Many technical difficulties need to be surmounted to make PMC's compatible with existing telecomm fiber technology, such as splicing HC-PCFs to step-index fibers [37, 45, 46], and reducing Fresnel back-reflection at glass-gas interfaces [47]. Here, two photonic microcells of sealed HC-PCFs, 1-cell kagome and 7-cell photonic bandgap, are explored to increase the portability and robustness of the system. Both the accuracy and stability of the portable frequency reference are characterized by analysis of an optical heterodyne beat with a frequency comb referenced to a GPS-disciplined Rb oscillator.

2. Improving characterization of accuracy and stability
In our previous work, a 10 kHz accuracy frequency measurement on an acetylene transition inside a hollow fiber vacuum chamber reference was demonstrated [8], and a stability of $1.2{\times}10^{-11}$ at 1s gate time was achieved. The experimental setup for frequency modulation (FM) SAS is shown in Fig. 7a. The modifications shown in Fig. 7b are discussed in Section 5.

   A 19-cell kagome HC-PCF, with a maximum core diameter of 68 μm and a length of 4.1 m, lies between two vacuum chambers. These vacuum chambers are evacuated with a vacuum pump and then filled with $^{12}C_2H_2$. A narrow linewidth continuous-wave (CW) fiber laser (Orbits Lightwave, Inc.) is used in this experiment to observe the P(13) $v_1 + v_3$ overtone transition in $^{12}C_2H_2$. The power from the fiber laser is split into a probe beam and a pump beam amplified by an erbium doped fiber amplifier (EDFA) up to 200 mW. The probe beam goes through an acousto-optic modulator (AOM) so that the interference between the probe and the reflected pump occurs at the AOM modulation frequency ($f_{AOM} \approx -60\ MH$). Then an electro-optic modulator (EOM) is used to create sidebands spaced at the EOM modulation frequency ($f_{EOM} = 22MHz$) for FM spectroscopy [48]. The probe beam exiting the kagome fiber is separated from the pump by a polarizing beam splitter, and is detected by a 125 MHz photoreceiver. The pump beam is amplitude modulated at 900 kHz for background noise rejection. By applying a ramp voltage to the piezo-electric transducer of the fiber laser, a sub-Doppler saturated absorption signal and antisymmetric error signal were observed as shown in Fig. 8.
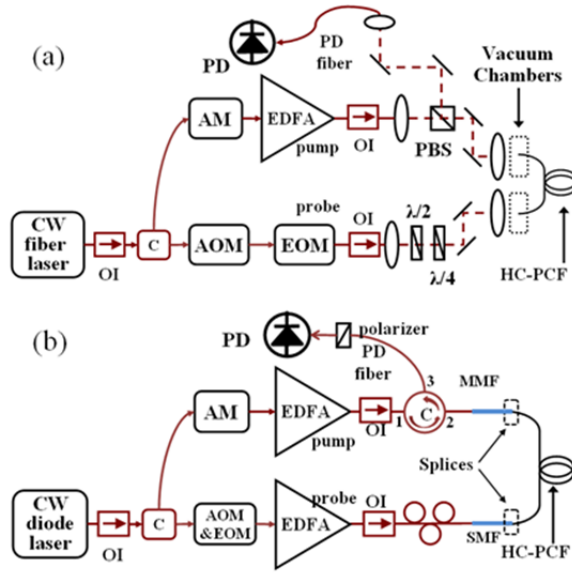
Fig. 7. Optical schematic of gas-filled hollow fiber frequency references based on (a) hollow core fiber between two vacuum chambers and (b) a sealed photonic microcell. Shown are amplitude modulator (AM), acousto-optic modulator (AOM), electro-optic modulator (EOM), polarizing beam splitter (PBS), optical isolator (OI), half waveplate (λ/2), quarter waveplate (λ/4), optical circulator (C), and photodetectors (PD).
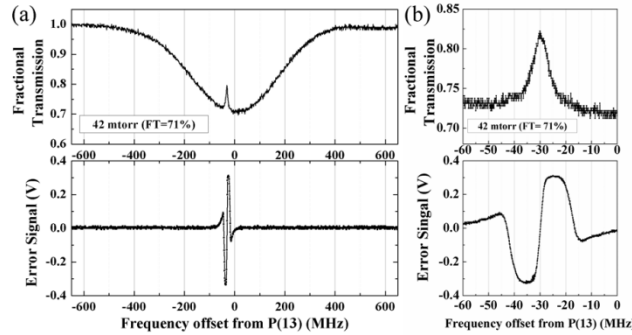

Fig. 8. (a) top: Fractional transmission of a 4.1 m long kagome HC-PCF with a $^{12}C_2H_2$ pressure of 42 mtorr, and a pump power of 25 mW exiting the fiber, bottom: error signal of sub-Doppler versus scanned frequency away from the P(13) transition. The laser frequency was scanned at 1.2 GHz/sec. (b) same as (a), but zoomed in on the sub-Doppler absorption feature.

Furthermore, the short-term stability and accuracy of this frequency reference were characterized [25]. A portion of the light split from the CW laser was used to beat with a phase stabilized carbon nanotube fiber laser (CNFL) frequency comb [26], which is referenced to a GPS-disciplined Rb oscillator. This RF beat frequency was recorded by a 12-digit counter, fractional Allan deviations were calculated and a stability of 1.2×10^{-11} at 1s sample period was obtained. Since the frequency stability of the beat between references is determined by the least stable one, previously [25] the measured short-term stability of our fiber reference was limited by the GPS-disciplined Rb oscillator, which provides the referencing signal for phase stabilizing the CNFL frequency comb.

2.1 Three-cornered hat to estimate individual stabilized laser stability
To better characterize the short-term stability in comparison to Ref.[25], we locked a second laser to a nearly duplicate gas-filled fiber and compared them. Because of equipment availability, one lock was not as robust as the other, and consequently we used a well know three-cornered hat method [49] to extract the stabilities of each reference. To obtain our best reference stability, we measured the beatnote between the CNFL comb and two stabilized fiber lasers (Fig. 3a) [50]. The counter gate time equals the sample period (τ) for τ ≤ 1s, and sample periods > 1s are realized by averaging. The fiber lasers are independently

locked to the $^{12}C_2H_2$ P(13) transition in two separate kagome-structured HC-PCFs vacuum chamber references. Figure 9b shows the fractional instability of two lasers beating of this work, and compared with the individual stability of other reported acetylene stabilized lasers realized in free-space gas cells [34, 51]. Under the assumption that the reference are uncorrelated, we calculated the stability of the individual laser (laser 1 and 2), as shown in Fig. 9b. Even though our acetylene linewidth is a factor of 10 broader than the gas cell setup [34, 51], the stability of our fiber-based reference is still comparable to those results. Furthermore, a stability of 2×10^{-12} (laser 2) at 0.1 s of our fiber-based acetylene frequency reference is obtained. To our knowledge, this performance approaches the best short-term stability achieved in acetylene frequency references [51].
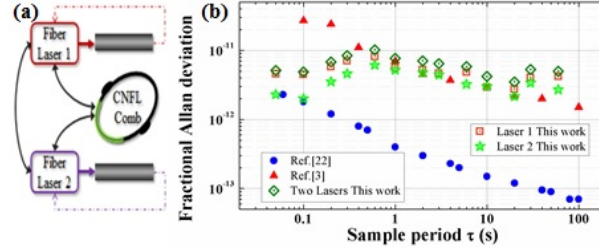

Fig. 9. (a) Schematic of the three-cornered hat measurement between two acetylene-stabilized fiber lasers and a phase stabilized CNFL comb. (b) Fractional Allan deviation of beat frequency between two acetylene-stabilized fiber lasers, compared with Ref. [51] and Ref. [34]. The individual stability of each laser obtained from three-cornered hat measurement is also shown.

3. FM modeling of frequency shift due to line-shape

While our previous measurement agreed with other published values within 1σ [43, 44], further investigation reveals distorted line-shape due to the frequency difference introduced by an AOM between the pump and probe beam. This distortion creates an additional shift at the kHz level which can be calculated by extending the FM modeling describe in Ref. [42], as described below.

The Pound-Drever-Hall (PDH) locking technique used in SAS depends on the complete information of the amplitude and phase shift on the carrier and two modulated sidebands (± 22 MHz). The amplitude information can be obtained from the theoretical line profiles of the Doppler and sub-Doppler features [52] and our measured absorption curve, by using the Kramers–Kronig relations.

The phase shift (φ) can be derived from the attenuation coefficient (δ) based on the spectral hole burnt by the unshifted pump.

$$\varphi(\omega) = -\frac{1}{\pi}P\int_{-\infty}^{\infty}\frac{\delta(\omega')}{\omega'-\omega}d\omega'$$

(1)

In the absolute frequency measurement of the frequency reference, when there is only a probe beam, the attenuation coefficient of the Doppler-broadened absorption is given as

$$\delta_D(\omega) = \frac{1}{2}\cdot A_g \cdot Exp\left[-\frac{(\omega+2\pi\cdot0.5f_{AOM})^2}{0.6\cdot\omega_D^2}\right]$$

(2)

where A_g is the amplitude of the Doppler absorption, ω_D is the Doppler linewidth, and f_{AOM} is the frequency shift of the probe beam from the laser frequency.

In the presence of the pump, the attenuation coefficient is given by Eq. (2) multiplied by a Lorentzian, resulting in

$$\delta(\omega) = \delta_D(\omega)\cdot\left(1-\frac{A_l}{R^2[\omega]+1}\right)$$

(3)

where R[ω] is a normalized frequency given by the expression

$$R[\omega] = \frac{\omega}{2\pi f_l/2}$$

$$(4)$$

Here, A_l is the amplitude of sub-Doppler absorption, and f_l is the sub-Doppler linewidth of the P(13) transition of $^{12}C_2H_2$.

In Equations (2, 3) above, $\omega_D = 470\ MHz$ is calculated from the Doppler-broadened width of the P(13) line of $^{12}C_2H_2$, f_l is the linewidth of the sub-Doppler (Lorentzian) feature, and the parameters A_g and A_l are related to the fractional transmission and pump power measured in the spectroscopy. The typical values of A_g=0.69 and $A_l = 0.3$ are for a signal with a 50% fractional transmission (FT), and with 32 mW pump power exiting the fiber.

Following the derivation in Ref. [42] with a sidebands' index of 0.1, the dispersive error signal of FM spectroscopy was calculated with and without the presence of the pump beam (pump-on and pump-off). By subtracting the error signal with pump off from the error signal with pump on, the residual error signal after amplitude modulating the pump beam was obtained. In Fig. 10, the calculated absorption and the SAS error signal at the P(13) line of $^{12}C_2H_2$ are shown (FT=50%, P_{pump}=32 mW).
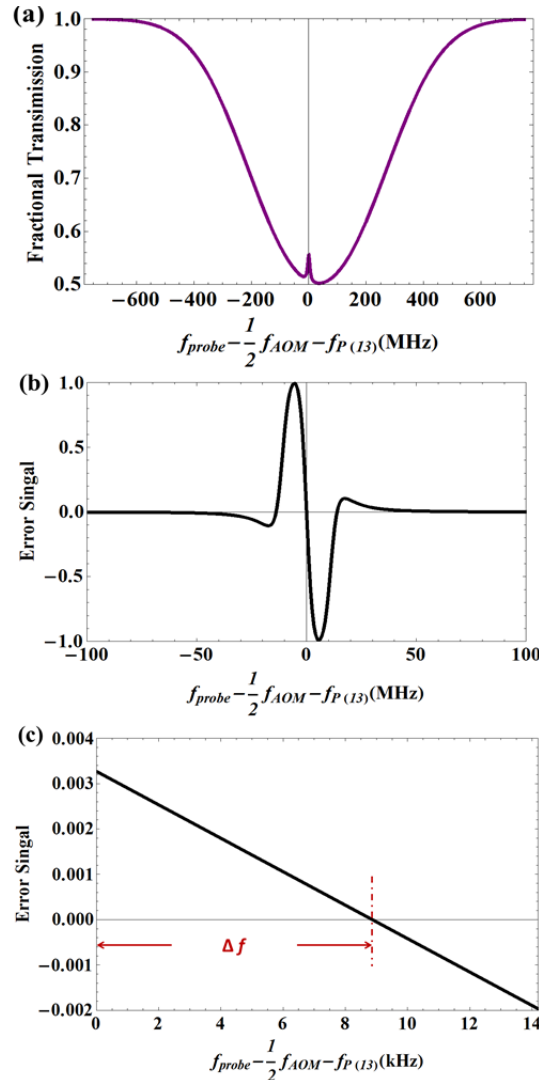

Fig. 10 (a) The calculated SAS of P(13) line of $^{12}C_2H_2$, with a FT of 50%, and exiting fiber pump power of 32 mW; (b) the normalized dispersive error signal of the P(13) line. The calculated error signal is proportional to what is detected by the PD; (c) same as (b) but plotted over smaller range to show the frequency of the zero-crossing.

In Fig. 10c, it is clear that the error signal crosses zero at a point shifted by $\Delta f = 9\ kHz$ from the zero of the x-axis. Previously [25] we took the measured laser frequency (f'_{meas}) to be $f'_{meas} = f_{v0,P} - \frac{1}{2}f_{AOM}$ where $f_{v0,p}$ is the frequency of the P(13) zero velocity class at the given pressure, and extrapolated to zero pressure to get the frequency of the P(13) line at zero pressure, here called $f'_{P(13)}$, as shown in Fig. 11.
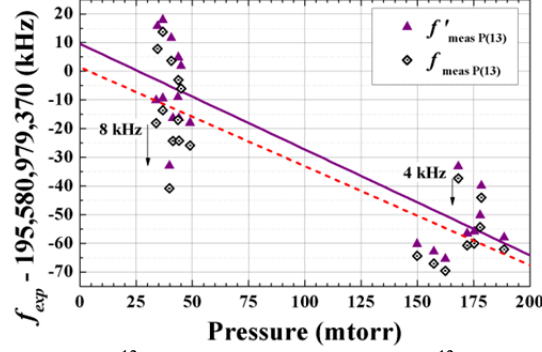

Fig. 11. Absolute frequency f_{exp} of the $^{12}C_2H_2$-stablized laser versus $^{12}C_2H_2$ pressure inside the 4.1 m long kagome fiber with a linear fit line. Solid triangle with solid linear fit line denotes absolute frequency before correction by Δf; open diamond with dash-dot linear fit indicates absolute frequency after correction by Δf: Each data point indicates an independent alignment to avoid frequency offsets due to free-space coupling into the kagome fiber. After applying the locking frequency shift, the linear fit gives a zero-pressure intercept of 195,580,979,371.4 ± 9.3 kHz, compared with the previously reported [25] zero-pressure intercept of 195,580,979,379.6 ± 9.3 kHz.

However, this analysis [25] neglects Δf. The corrected frequency of the P(13) line at zero pressure, called $f_{P(13)}$, must be corrected by applying the equation

$$f_{meas} = f_{v0,P} - \frac{1}{2}f_{AOM} - \Delta f = f'_{meas} - \Delta f$$

(5)

to each measurement, and extrapolating again.

This shift is due to the asymmetry of the sub-Doppler feature, which is caused by the frequency difference between the pump and probe beam arising because the probe frequency is shifted by the AOM. To validate this model experimentally, we made two measurements of the same absolute frequencies using two different AOMs; one shifts the probe frequency by ~ -60 MHz, and the other shifts the probe frequency by ~ 200 MHz. These two measurements were made under the same acetylene pressure, pump power and comb conditions. Figure 12 shows the calculated absolute frequency before (12a) and after (12b) applying this shift caused by the frequency difference of probe and pump beam. The measured absolute frequency of the same transitions before correction by Δf differed by 20±5 kHz while after the correction they differ by 5±5 kHz (ie. they agree).

The FM modeling was also applied to our previously reported absolute frequency measurement in a 4.1 m kagome HC-PCF [25] to make a correction of the measurement, as shown in Fig. 11; data were previously taken at two different pressure brackets in our absolute frequency measurements, and gave two different sets of parameters of A_g and A_l. So, here we reanalyzed these data by applying an 8 kHz shift to the lower pressure measurements, and a 4 kHz shift to the higher pressure measurements. A new fit to the shifted measurement yield a new measurement of the P(13) line in fiber that still agrees with the published value [43, 44] within the given error bar. The zero-pressure intercept of the kagome frequency reference adjust to 1.4 kHz, showing a better agreement with previous measurements of the P(13) line [43, 44], shown in Table 2.
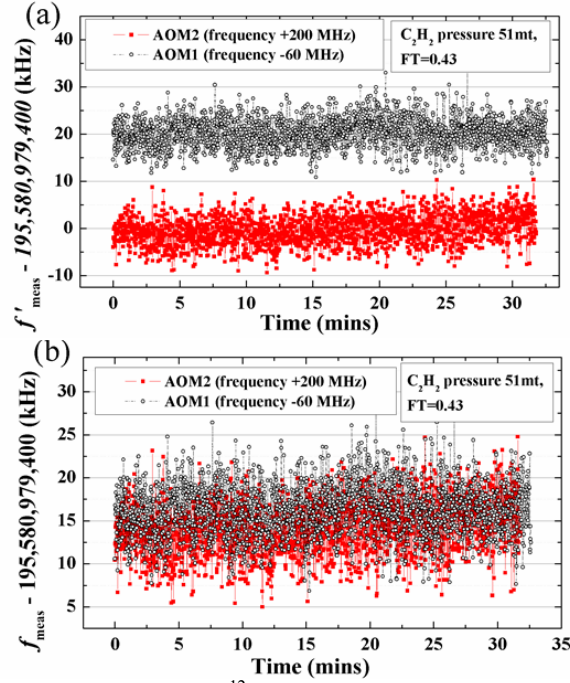
Fig. 12. Measured absolute frequency of the $^{12}C_2H_2$-stablized laser vs. time with a $^{12}C_2H_2$ pressure of 51 mtorr inside the 7.9 m-long kagome fiber, recorded at a 1s gate time using a counter: (a) before correcting for the shift caused by frequency difference between probe and pump, (b) after correction. Black open-circle: probe frequency was shifted by ~ -60 MHz with respect to the pump (AOM1), red solid-square: probe frequency was shifted by $\sim +200$ MHz with respect to the pump (AOM2).

Table 2. Mean $^{12}C_2H_2$ $\nu_1 + \nu_3$ P(13) frequency and uncertainty for this work (before[25], after considering the frequency shift Δf caused by FM modeling) and for referenced work [43, 44]
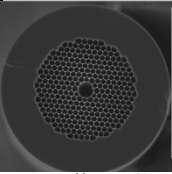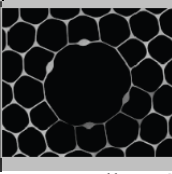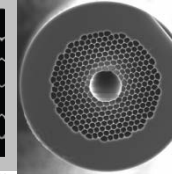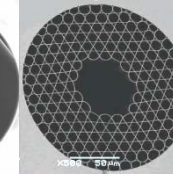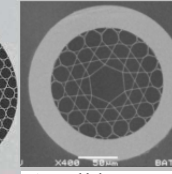
	Mean P(13) value (kHz)	Uncertainty (kHz)
This work after mod. Δf	195,580,979,371.4	9.3
This work before mod. Δf Ref. [25]	195,580,979,378.0	9.3
Ref. [43]	195,580,979,370.4	3.7
Ref. [44]	195,580,979,371.1	10.2

4. Suitable photonic crystal fibers for making PMCs

4.1 Surface mode modeling
Our previous work [25] establishes the 19-cell kagome photonic crystal fiber (PCF) as a suitable medium for precision spectroscopy of molecular gases. However, that fiber is difficult to splice with standard single mode fiber SMF-28 since the outer diameter of the 19-cell kagome PCF (305 μm) is roughly two times bigger than the outer diameter of SMF-28 (125 μm). While kagome fiber can be tapered and spliced to SMF [46], the best splice loss between the tapered large-core 19-cell kagome fiber and SMF is around 2 dB, which is higher than the 0.9 dB splice loss for a photonic bandgap PCF. Furthermore, these kagome-structured fibers are not yet commercially available. Therefore, we investigated three commercially available HC-PCFs for use in the all-fiber PMC frequency references: 7-cell photonic bandgap fiber (PBGF), 7-cell polarization maintaining (PM) PBGF, and 19-cell PBGF, shown in Table 3 (Fiber A-C). Because of their similar outer diameters (~120 μm) compared with SMF-28 (125 μm), they have the potential to make acetylene-filled PMCs.

Table 3. Fiber parameters for the HC-PCF

#	A	B	C	D	E
Cross Section					
Fiber Name	7-cell PBG	PM 7-cell PBG	19-cell PBG	19-cell kagome	1-cell kagome
Part number	HC-1550-02	HC-1550-PM-01	HC19-1550-01	*	*
Core diameter	11 μm	11 μm	20 μm	70 μm	45 μm
Outer diameter	120 μm	120 μm	115 μm	315 μm	200 μm

*Fabricated by the Gas-phase photonic and microwave materials group (GPPMM)

To initially test these commercially available fibers, we used them for vacuum chamber references as in Fig. 7a; both the stability and accuracy of the acetylene P(13) transition line are measured and calibrated. Fig. 13 shows the calculated fractional Allan deviation of these $^{12}C_2H_2$-filled PBGF references. The 20 μm PBGF (Fiber C) exhibits a factor of 2 worse stability than our previous kagome reference (Fiber D) [25] at 1s sample period, which is due to the smaller core-size of the PBGF and therefore larger - linewidth (due to transit time broadening). As for the 10 μm PBGF (Fiber A), we predicted a stability shown as solid triangles in Fig. 13 by scaling the stability offered at 1 s in large-core kagome to the smaller signal to noise (S/N) ratio and larger linewidth. Even so, the 10 μm PBGF observed in the measured fractional Allan deviation is a factor of 4 worse than the expected value.
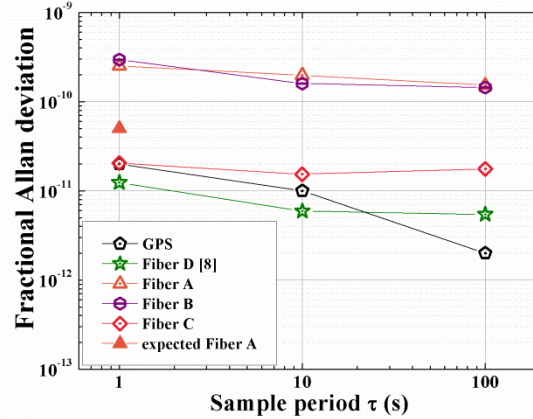

Fig. 13. Fractional instability of the beat between the frequency comb and the fiber-based acetylene reference made with different HC-PCFs shown in table I (Fiber A-D), GPS stability is shown here for comparison.

To explain this degraded S/N ratio, we observed that the 10 μm PBGF (Fiber A, B) exhibits large surface mode effects. Surface modes refer to a collection of modes guided in the glass region between the core and cladding [53], *i.e.* the core surround. These modes have higher loss and wavelength-dependent coupling to the core modes. Strong coupling to these can result in wavelength-dependent loss in the fibers, as shown in Ref. [54]. The frequency instability may be higher than expected due to these surface modes, which contribute a 40% variation in off-resonant transmitted power in the 10 μm PBGF (Fiber A, B) offered here. By comparison, the variation in the 20 μm core fiber (Fiber C) is only 5%, while that in large-core kagome is less than 1%. These surface modes may not only contribute an oscillating background [54], but may also corrupt a quantitative analysis of the line-shape [55].

Indeed, in fibers with strong wavelength-dependent transmission, we also observe an intensity dependent frequency shift of around 500 kHz in the error signal along with a highly asymmetric trace, which is obtained by Pound-Drever-Hall style modulation as described above. Such background should

be rejected by pump amplitude modulation. Thus the "survival" of the off-resonant transmission modulation to the error signal is at first surprising. The asymmetry (A) of the error signal is defined as

$$A = \frac{V_1 - V_2}{(V_1 + V_2)/2}$$

(6)

where V_1 and V_2 are the absolute value of the maximum and minimum voltages of the error signal.

To investigate the effect of the coupling between a core mode and surface modes, we consider the simple case where the coupling occurs only between a single core mode and a single surface mode. In this case the probe signal at the photoreceiver can be written in the following manner

$$V_{PD} = V_{core} + V_{SM} + 2\sqrt{V_{core}V_{SM}}\cos(\Delta\Phi + \Delta\Phi_{NL})$$

(7)

where $\Delta\Phi = \Delta\beta L_{fib}$ is the phase due to the mode beating between the core mode and surface mode, $\Delta\beta$ is the difference in the propagation constant between the two modes and L_{fib} is the effective length of the fiber. $\Delta\Phi_{NL}$ is an additional phase that depends on the pump intensity and is caused by the Kerr effect. Ignoring the Kerr effect in the hollow core, the associated propagation constant difference that gives rise to this phase shift is $\Delta\beta_{NL} = n_2^{SM} I_{SM}(2\pi/\lambda)$.. Here the n_2^{SM} is the nonlinear refractive index of the silica core-surround and I_{SM} is the intensity of the surface mode which can be written as $I_{SM} = 0.4 P_{pump}/A_{eff}$. If one estimates the surface mode effective area A_{eff} to be on the order of $3 \times 10^{-11} cm^2$, which is an experiential value for a similar fiber taking into account the glass thickness of the fiber core and the near field intensity profile, and $n_2^{SM} = 3 \times 10^{-16} cm^2/W$, the induced frequency shift due to this nonlinear optical coupling is ~ 500 kHz. This 500 kHz agrees with the intensity dependent frequency shift in the error signal along with a highly asymmetric trace, calculated by adding a sinusoidal term to Eq.(2) to simulate the surface mode in the calculation. The period of the sinusoidal term is obtained by measuring the transmission signal of PBGF while scanning the input laser frequency. A of the theoretical signal is calculated by applying Eq. (6) to the theoretical error signal.

Furthermore, in addition to the frequency shift, the Kerr effect induces an intensity dependent coupling strength between the core mode and the surface mode, which renders the error signal asymmetry (A) dependent on the pump intensity. Figure 14 illustrates this through considering error signal shape evolution when the coupling of the core mode with the surface modes is considered or not. A of both theoretical and experimental curves is calculated by applying Eq. (6) to the plotted error signal (Fig. 14a and 14b). The calculated error signal exhibits very little asymmetry when the surface mode is neglected or when only $\Delta\Phi$ is considered. However, when $\Delta\Phi_{NL}$ is included, the experimentally observed (Fig. 14b) asymmetry of 20% is obtained theoretically (Fig. 8a). This arises because the pump beam intensity changes the surface mode as it is modulated, so that pump amplitude modulation does not reject the signal due to the surface mode.
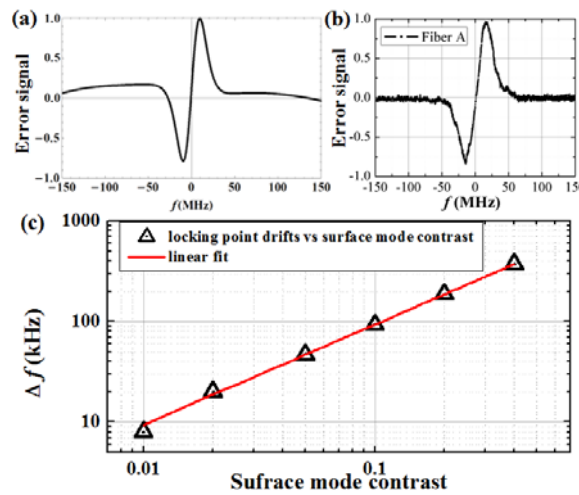

Fig. 14. (a) Calculated error signal in acetylene-filled 10 μm PBGF with the nonlinear effect caused by pump power modulation; (b) experimental error signal; (c) Calculated maximum locking frequency change verse different surface mode contrast when varying only $\Delta\Phi$ (not $\Delta\Phi_{NL}$) by π to mimic slow thermal drift.

   Even without taking into account the change of $\Delta\Phi_{NL}$ caused by the pump modulation, a slow thermal drift in $\Delta\Phi$ will introduce a frequency shift of up to 373 kHz when a 40% contrast surface mode is present (Fig. 14c). Therefore it is clear that very small changes in the surface mode will lead to changes in the lock point, causing frequency instability (Fig.13) and inaccuracy.

4.2 Polarization maintaining fiber
Polarization-maintaining fiber was also explored to improve the reference. This is motived by the observation of a 40 kHz shift [56] when the probe polarization is changed by 30^0. This shift is considerable compared with the 10 kHz accuracy obtained in the kagome reference, and polarization may limit the accuracy of a gas-filled photonic microcell reference. One possible solution is to use polarization maintaining (PM) HC-PCF to make gas-filled microcell references. The commercially available 7-cell PM HC-PCF (Fiber B in Table II) from NKT Photonics was tested, and a stability of 3.0×10^{-10} at 1 s sample period has been achieved (Fig. 13). In the experiment, a linear film polarizer was placed before the vacuum chamber on the probe arm to guarantee a linearly polarized probe beam, and a half waveplate was placed after the polarized beam to adjust the polarization of the probe beam coupled into the fiber. To find the polarization maintaining axis of the PM fiber, the extinction ratios of the probe beam exiting the fiber are measured (Fig. 15a) at different probe polarization angles. The maximum contrast ratio indicates that the probe beam is coupled into either the fast or slow axis of the PM fiber, and thus polarization is preserved when the beam is travelling through the fiber. Beat frequencies were measured when the probe beam was coupled into each axis and ~ 1 MHz shift in the average values of beat frequencies was observed. A possible explanation is this PM fiber has different wavelength-dependent transmission near the fast and slow axis, or the surface mode exhibits polarization dependence.
   By coupling the probe to the 88^0 axis, which is the fast or slow axis (Fig. 15a), the absolute frequency measurements (Fig. 15b) were investigated at three different pressure ranges. The results gave us ~ 1 MHz uncertainty in each frequency range, and beatnote frequency excursions on the 15 minutes time scale (*i.e.* "beatnote noise") of up to 0.5 MHz were detected (the error bar on Fig. 15b). Linear fitting is applied to the data, and gives the absolute frequency after accounting for power shift and pressure shift. The uncertainty reflected in the gas-filled PM fiber reference is thought to be due to the effect of surface modes we discussed above, and result in a frequency reference with only 1 MHz accuracy at best.
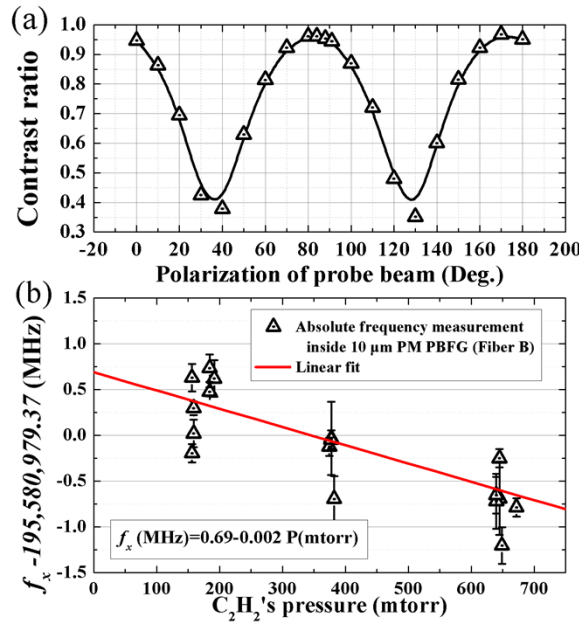

Fig. 15 (a) Contrast ratio of probe power exiting fiber vs. the angle of probe polarization in vacuum, solid line fitting curve of measured data, (b) Absolute frequency measurement of $^{12}C_2H_2$ P(13) line inside 10 μm PM PBGF (Fiber B); zero frequency corresponds to the published value [44] .

5. Sealed photonic microcells

To eliminate the -vacuum chambers, gas is sealed inside the PCFs, creating photonic microcells (PMC's) [37, 45, 46]. To explore the stability and accuracy of the sealed PMC, the setup shown in Fig. 7b is used. We increase the portability of the frequency reference and hopefully can reduce the sensitivity of the reference to alignment of the fiber into the vacuum setup [25]. In the experiment, a narrow linewidth CW laser near 1.5 μm is split by a fiber coupler to generate a frequency modulated probe beam and an amplitude modulated pump beam. Also the AOM is used to shift the interference between the probe and the reflected pump to the AOM frequency, which can then be filtered away, while the EOM is used to create sidebands spaced at the modulation frequency for FM spectroscopy [48]. The pump, counter-propagating with the probe, passes through an EDFA to saturate the acetylene molecules. Since loss is introduced during the two splices, another EDFA is used to increase the probe power coupled into the PMC. In addition, a fiber circulator is used to separate the probe and pump beams, and the resulting probe beam is detected by a photoreceiver. The remaining CW light from the laser beats against a phase stabilized CNFL frequency comb [26] to characterize the stability and accuracy of the reference. The RF beat frequency is recorded by counters with a 1 s gate time.

Two photonic microcells are tested in our experiment. One microcell is made of a 10 μm PBGF (Fiber A) microcell, with a length of 4 m and a pressure of 174 mtorr, causing 22% transmission on the P(13) line by the CW fiber laser used in the kagome setup (Fig. 7a). A ramp voltage scans the laser frequency linearly in time to calibrate the linewidth and S/N ratio of the error signal. The typical linewidth is 17 MHz with a pump power of 16 mW, and the S/N ratio is ~7, which is mainly due to the pump reflection at the splice interface between PBGF and SMF and the surface mode in the 10 μm PBGF. A 1.5 MHz beatnote noise (Fig. 10a) is measured in the P(13) v_1+v_3 overtone transition of acetylene inside this 10 μm PBGF microcell.
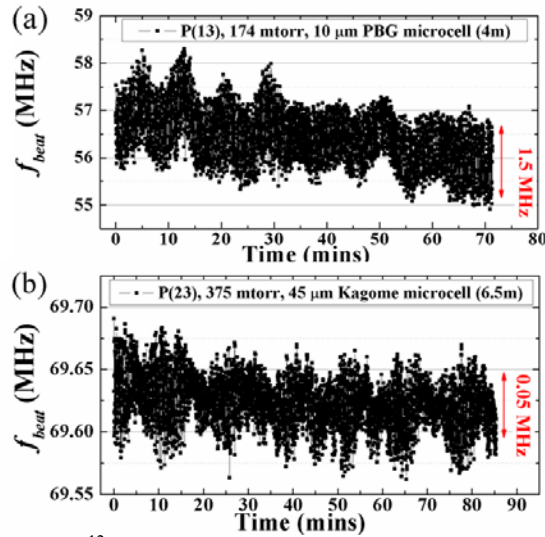

Fig. 16 (a) Beat frequency vs. time in $^{12}C_2H_2$-filled 10 μm PBGF PMC for the P(13) line transition, (b) beat frequency vs. time in $^{12}C_2H_2$-filled 45 μm kagome PMC for the P(23) line transition.

The other particular microcell, made of a 1 cell kagome (Fiber E), was originally built for an electromagnetically induced transparency measurement, with a length of 6.5 m and a pressure of 375 mtorr [46], which leads to a 100% fractional absorption on the P(13) line. Therefore, a tunable diode laser (Santec TSL-210) is tuned to 1539 nm with 6 mW optical power to measure a weaker line, P(23), which gives a fractional absorption of 76%. An error signal is generated with a factor of 2 worse linewidth and a factor of 10 worse S/N ratio compared to what is observed in large-core kagome vacuum chamber reference [25]. This particular 1 cell kagome PMC gives beatnote frequency excursions on the time scale of ~15 minutes (*i.e.* "beatnote noise") around 50 kHz and a diode laser is stably locked to this PMC over 80 minutes (Fig. 10b).

As shown in Fig. 17, the fractional instabilities of those two microcells beatnote measurements are also calculated. The long-term instability of both PMC-locked lasers may be caused by the drift of the probe polarization mentioned earlier in this paper. The fractional instability at 1 s averaging gate time is worse

than that of our vacuum chamber reference setup [25]. For the PBG microcell, the fractional stability at 1s is dominated by the broadened linewidth, pump reflections, and the surface modes in PBGF PMC, while for the kagome microcell, the fractional stability is mainly caused by broadened linewidth, pump reflections and the noisier laser.
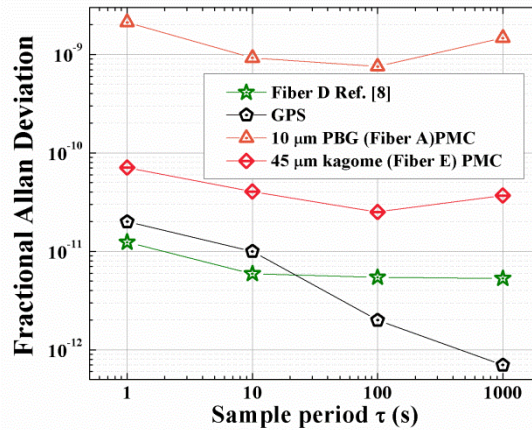

Fig. 17 Fractional instability vs. averaging time in two PMCs: P(13) line of $^{12}C_2H_2$ PBGF PMC and P(23) line of $^{12}C_2H_2$ kagome PMC.

We also explored the environmental sensitivity of the kagome PMC-locked laser. In the measurement, the kagome PMC is put in a cardboard box with a lid. Several actions are applied to this particular microcell, such as opening the box, shaking the box, pressing on the PMC, and changing polarizations of the probe and pump beams. A shift of up to 1.2 MHz occurs when we shake the box, and a shift of up to 1 MHz is caused by changing the probe polarization. Fortunately, all those shifts are reversible. The beat frequency returned to its original value (± 0.05 MHz) after all the actions applied on the PMC were set to the beginning states.

Here, we track the performance of the PMC reference over an extended period of time. As shown in Fig. 18a, the long-term stability is improved by using a polarization maintaining (PM) erbium doped fiber amplifier (EDFA) (red triangles) to amplify the probe beam power instead of a non-PM EDFA (yellow squares and cyan hexagons). We also notice a factor of 2 degradation in the stability after six months compared to our initial data, but no further degradation was observed. The degradation may be caused by outgassing of contaminants in the PMC. We also found deterioration in the PBGF PMC after a delay of a year. Longer evacuation time and heating the HC-PCF before use may help to reduce any impurities in the inner core of the fiber. Even so, our PMC-stabilized acetylene frequency reference shows a reproducibility of ± 170 kHz on the P(23) line of $^{12}C_2H_2$ over 1 year. The P(23) line is measured to be 194,742,536,524±86kHz. Systematic shifts and uncertainties in this absolute frequency measurement arise due to pump power, residual gas pressure and temperature drifts. After the correction due to the pressure shift of - 0.393 MHz/torr [57], our measured P(23) frequency is 194,742,536,671 ± 86 kHz (1σ) (Fig. 18b), which agrees with a previous measurement in a power built-up cavity of 194,742,536,722.9 ± 1.8 kHz [44] within uncertainty.
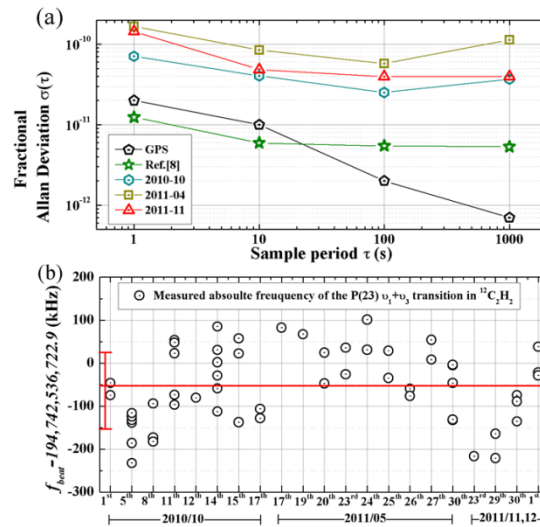
Fig. 18 (a) Fractional Allan Deviation of the beatnote between the fiber-based acetylene stabilized laser and the CNFL comb: cyan hexagons, yellow squares, and red triangles − P(23) line in sealed PMC at different dates; green star− P(13) line of acetylene filled large-core kagome HC-PCF in vacuum chamber; black pentagons− GPS-disciplined Rb oscillator. (b) Experimentally measured repeatability of the absolute frequency in the kagome PMC of the P(23) $v1+v3$ transition in $^{12}C_2H_2$ at a different date and time; red line− average value of measured absolute frequencies.

6. Summary

In this paper, we showed improvements in the characterization of our previously published results on acetylene frequency references in kagome fiber by obtaining higher short term stabilities; the absolute frequency agrees better with previously published values after modifying the shift due to the lineshape. Several commercially available HC-PCFs yield reduced accuracy and stability due to increased linewidths as anticipated, and also exhibit excess noise due to surface modes. Polarization maintaining fiber was used to fabricate a PMC, but the resulting reference was only good to ~ 1 MHz, indicating the need for PM fiber with reduced surface modes, such as the kagome fiber design. The poor performance of 7-cell photonic bandgap fiber was investigated, and led to a deeper understanding of the negative role of surface modes in the reference performance. Sealed Photonic microcells based on both PBGF and kagome fiber were characterized over a year, and demonstrate agreement with previously published values within ~ 100 kHz, which can be improved by better splice techniques.

These results have led us to focus our efforts to improve the photonic microcell frequency references on sealing large-core kagome fiber with angle splices, which may eliminate the negative effects of surface modes and reflections, and bring PMC performance in line with the superior accuracy and stability already observed in vacuum chamber based fiber references.

III. **Direct fiber comb stabilization to a gas-filled Single-moded hollow-core fiber for portable acetylene frequency reference**
     This material was previously published in Ref. [58].

1. Introduction

High-precision frequency references near 1.5 μm are desirable for optical telecommunications, optical sensing, metrology, and many other applications. 1 kHz accuracy acetylene frequency references have been created in free space and cavity configurations [34, 35] that require large containers to fulfill the required interaction lengths and high saturation intensities. The advent of gas-filled hollow-core photonic crystal fibers (HC-PCFs) [59] and their sealed form, the photonic microcell (PMC) [37], enable a portable and robust alternative to traditional gas-filled glass-cell-based molecular frequency standards [31]. Previously, we have explored several possible suitable PCFs for PMC fabrication, both photonic bandgap and kagome structured [31]. However, the highest signal-to-noise ratio (SNR) sub-Doppler signals are achieved in the largest core sizes (up to ~100 μm), whch are typically multi-mode and therefore suffer from mode-dependent frequency shift [31, 60]. This shift was observed as a sensitivity of the reference lock-point to optical alignment of the pump and probe beams into the fiber. Such modal frequency dependence may arise from sensitivity of sub-Doppler spectroscopy to wavefront curvature, and makes the portable frequency reference subject to environmental stresses such as thermal fluctuation and vibration, which cause mode missing within the fiber. Furthermore, photonic bandgap fibers typically have surface mode beating that creates instability in the frequency lock [31].

Here, we address these problems by employing the first hollow-core fiber employing Perturbed Resonance for Improved Single Modedness (PRISM) [61]. The saturated absorption spectroscopy (SAS) signal is observed to be devoid of unwanted surface mode effects, and reduced dependence of the reference on optical alignment is inferred from preliminary locking data. Toward PMC fabrication, we demonstrate robust splicing of the PRISM fiber to SMF-28 with both conventional and angle interfaces.

2. Saturated absorption for gas-filled PRISM fiber and alignment sensitivity

To initially test this PRISM fiber, we used it for vacuum chamber references as in Ref.[25]. A 10 m fiber is coiled to 5cm diameter to improve single modedness, and loaded with acetylene to a pressure of 50 mtorr. The narrow SAS signal shown in Fig. 19 a (< 10 MHz FWHM) is obtained with frequency and pump amplitude modulation, and shows no surface mode effects. The SNR of 30 is smaller than that in the kagome reference (~150) [8] due in part to larger transit-time linewidth, residual background pressure, and reduced pump power. To explore the sensitivity of the frequency lock point to optical alignment, we stabilize a cw laser to the absorption feature, and beat against a phase stabilized frequency comb. Previously [8], the frequency lock point changed by ~20 kHz when the probe power was reduced by a factor 2 using an attenuator, but by 100 kHz when the fiber coupling was altered enough to reduce the probe power by a factor of 2. Here, in a similar test shown in Fig. 1b the shift due to probe power alone is ~ 100 kHz, while the shift due to alignment is only 50 kHz. The factor 5 higher sensitivity to probe power may result from the 5 times smaller SNR. But the comparable sensitivity of the reference frequency to probe power and probe alignment may indicate a common cause, rather than frequency dependence on fiber mode. This test will be more conclusive when the SNR ratio in the PRISM fiber is increased.

This PRISM fiber is suitable for portable acetylene-filled frequency reference in a 10 m length. Since optimal single-modedness is expected at longer lengths (~10-30 m), a gas such as ammonia, with weaker absorption, requires higher pressure than acetylene, and therefore is less sensitive to residual background gas pressure, resulting in higher SNR.
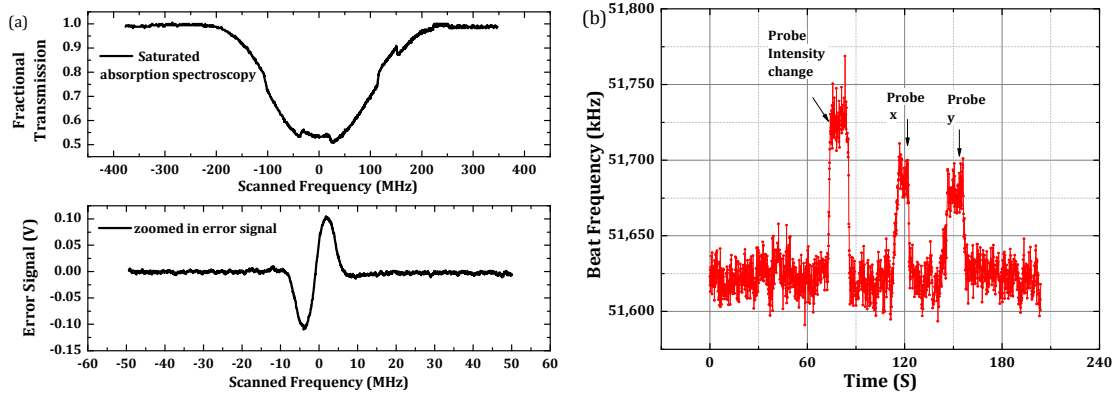
Fig. 19: (a) fractional transmission of P(13) inside PRIMS fiber vs. scanned frequency; bottom: zoomed in dispersion error signal of sub-Doppler vs. scanned frequency away from the P(13) transition. (b) Frequency shifts of the cw reference due to probe misalignment. The beat frequency between the frequency comb and the cw reference is plotted vs. time, x: horizontal mirror position; y: vertical mirror position.

3. Conventional and angle splice of PRISM fiber and SMF-28

To eliminate the vacuum chambers, we need to seal the gas inside the PRISM fiber, creating a PMC. A robust conventional splice of PRISM fiber and SMF-28 is achieved with a typical 2 dB splice loss using a Vytran-2000 fusion splicer. With both end spliced to SMF-28, the transmission loss though 20 m PRISM fiber coiled 5cm diameter is about 7.8 dB. To reduce the 4% Fresnel reflection that degrades the performance of the PMC-based frequency reference, both fibers are cleaved at an 8^0 angle before splicing; the splice loss increases to 3 dB but the return loss is reduced to -56 dB. With one end conventional spliced and the other end angle spliced to SMF-28, the transmission loss through the 20 m fiber is about 10 dB. Images of these splices are shown in Fig. 20.

Fig. 20: side-views of (a) a conventional splice and (b) an angle splice of PRISM fiber and SMF-28.

A gas-filled PMC based on angle-spliced PRISM fiber and SMF-28 may lead to improved frequency stabilization. We expect an improvement over the stability and accuracy of previously reported acetylene-filled PMC references [31]. This work dem08/2011onstrates that this PRISM fiber is promising for portable frequency references, and other accurate PMC-based devices.

References

1. S. Wu, C. Wang, C. Fourcade-Dutin, B. R. Washburn, F. Benabid, and K. L. Corwin, "Direct fiber comb stabilization to a gas-filled hollow-core photonic crystal fiber," Optics Express **22**, 23704-23715 (2014).
2. S. Wu, C. Wang, C. Fourcade Dutin, B. R. Washburn, F. Benabid, and K. L. Corwin, "Direct Comb Stabilization to a 12C2H2-filled Hollow-core Fiber via Single Tooth Saturated Absorption Spectroscopy," in *CLEO: 2014*(Optical Society of America, San Jose, California, 2014), p. SW1O.1.
3. S. Wu, C. Wang, C. Fourcade-Dutin, B. R. Washburn, F. Benabid, K. L. E. D. K. I. R. D. A. N. Corwin, and D. Hagan, "Direct Stabilization of a Frequency Comb to a 12C2H2-filled Hollow-core Photonic Crystal Fiber," in *Frontiers in Optics 2013*(Optical Society of America, Orlando, Florida, 2013), p. FTu1A.4.
4. S. Wu, C. Wang, C. Fourcade-Dutin, B. R. Washburn, F. Benabid, and K. L. Corwin, "Sub-Doppler Intrafiber Spectroscopy of C2H2 Using Amplified Frequency Comb Lines Directly," in *CLEO: 2013*(Optical Society of America, San Jose, California, 2013), p. CTu3I.1.
5. M. S. K. T. M. Fortier, F. Quinlan, J. Taylor, J. C. Bergquist, T. Rosenband, N. Lemke, A. Ludlow, Y. Jiang, C. W. Oates and S. A. Diddams, "Generation of ultrastable microwaves via optical frequency division," Nat. Photon. **5**, 425-429 (2011).
6. Y. Kim, S. Kim, Y.-J. Kim, H. Hussein, and S.-W. Kim, "Er-doped fiber frequency comb with mHz relative linewidth," Opt. Express **17**, 11972-11977 (2009).
7. L. C. Sinclair, I. Coddington, W. C. Swann, G. B. Rieker, A. Hati, K. Iwakuni, and N. R. Newbury, "Operation of an optically coherent frequency comb outside the metrology lab," Opt. Express **22**, 6996-7006 (2014).
8. D. Hou, J. Wu, S. Zhang, Q. Ren, Z. Zhang, and J. Zhao, "A stable frequency comb directly referenced to rubidium electromagnetically induced transparency and two-photon transitions," Appl. Phys. Lett. **104**, - (2014).
9. D. C. Heinecke, A. Bartels, T. M. Fortier, D. A. Braje, L. Hollberg, and S. A. Diddams, "Optical frequency stabilization of a 10 GHz Ti:sapphire frequency comb by saturated absorption spectroscopy in ^{87}rubidium," Phys. Rev. A **80**, 053806 (2009).
10. Y. I. S. Yamashita, K. Hsu, T. Kotake, H. Yaguchi, D. Tanaka, M. Jablonski, S.Y. Set, "5-GHz pulsed fiber Fabry-Perot laser mode-locked using carbon nanotubes," IEEE Photon. Technol. Lett. **17**, 750-752 (2005).
11. L. N. J. J. McFerran, W. C. Swann, J. B. Schlager and N. R. Newbury, "A passively mode-locked fiber laser at 1.54 mum with a fundamental repetition frequency reaching 2 GHz.," Opt. Express **15**, 13155-13166 (2007).
12. M. Akbulut, J. Davila-Rodriguez, I. Ozdur, F. Quinlan, S. Ozharar, N. Hoghooghi, and P. J. Delfyett, "Measurement of carrier envelope offset frequency for a 10 GHz etalon-stabilized semiconductor optical frequency comb," Opt.Express **19**, 16851-16865 (2011).
13. D. Mandridis, C. Williams, I. Ozdur, and P. J. Delfyett, "Low noise chirped pulse mode-locked laser using an intra-cavity Fabry-Pérot etalon," Opt. Express **19**, 8994-8999 (2011).
14. J. Chen, J. W. Sickler, P. Fendel, E. P. Ippen, F. X. Kärtner, T. Wilken, R. Holzwarth, and T. W. Hänsch, "Generation of low-timing-jitter femtosecond pulse trains with 2 GHz repetition rate via external repetition rate multiplication," Opt. Letters **33**, 959-961 (2008).

15. D. Chao, M. Sander, G. Chang, J. Morse, J. Cox, G. Petrich, L. Kolodziejski, F. Kaertner, and E. Ippen, "Self-referenced Erbium Fiber Laser Frequency Comb at a GHz Repetition Rate," in *Optical Fiber Communication Conference* (Optical Society of America Los Angeles, California, 2012), p. OW1C.2.

16. D. K. a. O. Gat, "Phase-coherent repetition rate multiplication of a mode-locked laser from 40 MHz to 1 GHz by injection locking," Opt. Express **20** 2717–2724 (2011).

17. P. Del'Haye, K. Beha, S. B. Papp, and S. A. Diddams, "Self-Injection Locking and Phase-Locked States in Microresonator-Based Optical Frequency Combs," Physical Review Letters **112**, 043905 (2014).

18. G. Y. F. Quinlan, S. Osterman, and S. Diddams, "A 12.5 GHz-Spaced Optical Frequency Comb Spanning >400 nm for near-Infrared Astronomical Spectrograph Calibration," Rev. Sci. Instrum. **81**, 063105 (2010).

19. T. Steinmetz, T. Wilken, C. Araujo-Hauck, R. Holzwarth, T. W. Hänsch, L. Pasquini, A. Manescau, S. D'Odorico, M. T. Murphy, T. Kentischer, W. Schmidt, and T. Udem, "Laser Frequency Combs for Astronomical Observations," Science **321**, 1335-1337 (2008).

20. F. C. Cruz, M. C. Stowe, and J. Ye, "Tapered semiconductor amplifiers for optical frequency combs in the near infrared," Opt. Lett. **31**, 1337-1339 (2006).

21. H. S. Moon, H. Y. Ryu, S. H. Lee, and H. S. Suh, "Precision spectroscopy of Rb atoms using single comb-line selected from fiber optical frequency comb," Opt. Express **19**, 15855-15863 (2011).

22. R. Laming, M. N. Zervas, and D. N. Payne, "Erbium-doped fiber amplifier with 54 dB gain and 3.1 dB noise figures," IEEE Photon. Technol. Lett. **4**, 1345-1347 (1992).

23. R. I. Laming, and D. N. Payne, "Noise characteristics of erbium-doped fiber amplifier pumped at 980 nm," IEEE Photon. Technol. Lett. **2**, 418-421 (1990).

24. F. B. a. P. J. Roberts, "Linear and nonlinear optical properties of hollow core photonic crystal fiber," Journal of Modern Optics **58**, 87-124 (2011).

25. K. Knabe, S. Wu, J. K. Lim, K. A. Tillman, P. S. Light, F. Couny, N. Wheeler, R. Thapa, A. M. Jones, J. W. Nicholson, B. R. Washburn, F. Benabid, and K. L. Corwin, "10 kHz accuracy of an optical frequency reference based on (C2H2)-C-12-filled large-core kagome photonic crystal fibers," Opt. Express **17**, 16017-16026 (2009).

26. J. Lim, K. Knabe, K. A. Tillman, W. Neely, Y. Wang, R. Amezcua-Correa, F. Couny, P. S. Light, F. Benabid, J. C. Knight, K. L. Corwin, J. W. Nicholson, and B. R. Washburn, "A phase-stabilized carbon nanotube fiber laser frequency comb," Opt. Express **17**, 14115-14120 (2009).

27. K. Tamura, E. P. Ippen, H. A. Haus, and L. E. Nelson, "77-fs pulse generation from a stretched-pulse mode-locked all-fiberring laser," Opt. Lett. **18**, 1080-1082 (1993).

28. Y. Y. Wang, N. V. Wheeler, F. Couny, P. J. Roberts, and F. Benabid, "Low loss broadband transmission in hypocycloid-core Kagome hollow-core photonic crystal fiber," Opt. Lett. **36**, 669-671 (2011).

29. E. D. Black, "An introduction to Pound-Drever-Hall laser frequency stabilization," Am. J. Phys. **69**, 9 (2001).

30. C. Wang, N. V. Wheeler, C. Fourcade-Dutin, M. Grogan, T. D. Bradley, B. R. Washburn, F. Benabid, and K. L. Corwin, "Acetylene frequency references in gas-filled hollow optical fiber and photonic microcells," Appl. Opt. **52**, 5430-5439 (2013).

31. C. Wang, N. V. Wheeler, C. Fourcade-Dutin, M. Grogan, T. D. Bradley, B. R. Washburn, F. Benabid, and K. L. Corwin, "Acetylene frequency references in gas-filled hollow optical fiber and photonic microcells," Appl. Opt. **52**, 5430-5439 (2013).

32. A. Czajkowski, A. A. Madej, and P. Dubé, "Development and study of a 1.5 µm optical frequency standard referenced to the P(16) saturated absorption line in the ($v_1 + v_3$) overtone band of $^{13}C_2H_2$," Optics Communications **234**, 259-268 (2004).

33. H. S. Moon, W. K. Lee, and H. S. Suh, "Absolute-Frequency Measurement of an Acetylene-Stabilized Laser Locked to the P(16) Transition of $^{13}C_2H_2$ Using an Optical-Frequency Comb," Instrumentation and Measurement, IEEE Transactions on **56**, 509-512 (2007).

34. P. Balling, M. Fischer, P. Kubina, and R. Holzwarth, "Absolute frequency measurement of wavelength standard at 1542nm: acetylene stabilized DFB laser," Opt. Express **13**, 9196-9201 (2005).

35. M. de Labachelerie, K. Nakagawa, and M. Ohtsu, "Ultranarrow $^{13}C_2H_2$ saturated-absorption lines at 1.5 µm," Opt. Lett. **19**, 840-842 (1994).

36. F. Benabid, J. C. Knight, G. Antonopoulos, and P. S. J. Russell, "Stimulated Raman Scattering in Hydrogen-Filled Hollow-Core Photonic Crystal Fiber," Science **298**, 399-402 (2002).

37. F. Benabid, F. Couny, J. C. Knight, T. A. Birks, and P. S. J. Russell, "Compact, stable and efficient all-fibre gas cells using hollow-core photonic crystal fibres," Nature **434**, 488-491 (2005).

38. F. Couny, P. S. Light, F. Benabid, and P. S. J. Russell, "Electromagnetically induced transparency and saturable absorption in all-fiber devices based on $^{12}C_2H_2$-filled hollow-core photonic crystal fiber," Optics Communications **263**, 28-31 (2006).

39. V. Ahtee, M. Merimaa, and K. Nyholm, "Fiber-Based Acetylene-Stabilized Laser," Instrumentation and Measurement, IEEE Transactions on **58**, 1211-1216 (2009).

40. A. Lurie, C. R. Locke, C. Perrella, P. S. Light, F. Benabid, and A. N. Luiten, "Towards a compact optical fibre clock," in *Precision Electromagnetic Measurements (CPEM), 2010 Conference on*(2010), pp. 16-17.

41. A. M. Cubillas, J. Hald, and J. C. Petersen, "High resolution spectroscopy of ammonia in a hollow-core fiber," Opt. Express **16**, 3976-3985 (2008).

42. G. C. Bjorklund, M. D. Levenson, W. Lenth, and C. Ortiz, "Frequency modulation (FM) spectroscopy," Applied Physics B: Lasers and Optics **32**, 145-152 (1983).

43. C. S. Edwards, G. P. Barwood, H. S. Margolis, P. Gill, and W. R. C. Rowley, "High-precision frequency measurements of the $v_1 + v_3$ combination band of $^{12}C_2H_2$ in the 1.5 µm region," Journal of Molecular Spectroscopy **234**, 143-148 (2005).

44. A. A. Madej, A. J. Alcock, A. Czajkowski, J. E. Bernard, and S. Chepurov, "Accurate absolute reference frequencies from 1511 to 1545 nm of the $v_1 + v_3$ band of $^{12}C_2H_2$ determined with laser frequency comb interval measurements," J. Opt. Soc. Am. B **23**, 2200-2208 (2006).

45. F. Benabid, P. S. Light, and F. Couny, "Low insertion-loss (1.8 dB) and vacuum-pressure all-fiber gas cell based on Hollow-Core PCF," in *Lasers and Electro-Optics, 2007 and the International Quantum Electronics Conference. CLEOE-IQEC 2007.*(2007), pp. 1-1.

46. N. V. Wheeler, M. D. W. Grogan, P. S. Light, F. Couny, T. A. Birks, and F. Benabid, "Large-core acetylene-filled photonic microcells made by tapering a hollow-core photonic crystal fiber," Optics Letters **35**, 1875-1877 (2010).

47. F. Couny, F. Benabid, and P. S. Light, "Reduction of Fresnel Back-Reflection at Splice Interface Between Hollow Core PCF and Single-Mode Fiber," Photonics Technology Letters, IEEE **19**, 1020-1022 (2007).

48. J. L. Hall, L. Hollberg, T. Baer, and H. G. Robinson, "Optical heterodyne saturation spectroscopy," Applied Physics Letters **39**, 680-682 (1981).

49. J. E. Gray, and D. W. Allan, "A Method for Estimating the Frequency Stability of an Individual Oscillator," in *28th Annual Symposium on Frequency Control. 1974*(1974), pp. 243-246.

50. C. Wang, N. V. Wheeler, C. F. Dutin, M. Grogan, T. Bradley, B. R. Washburn, F. Benabid, and K. L. Corwin, "Accurate Fiber-based Acetylene Frequency References," in *Conference on Lasers and Electro-Optics* (Optical Society of America, San Jose, CA, 2012), p. CF2C.7.

51. J. Hald, L. Nielsen, J. C. Petersen, P. Varming, and J. E. Pedersen, "Fiber laser optical frequency standard at 1.54 μm," Opt. Express **19**, 2052-2063 (2011).

52. W. Demtroder, "Laser spectroscopy : basic concepts and instrumentation / Wolfgang Demtroder," in *Springer series in chemical physics ; v. 5*(Springer-Verlag, Berlin ; New York :, 1981).

53. J. West, C. Smith, N. Borrelli, D. Allan, and K. Koch, "Surface modes in air-core photonic band-gap fibers," Opt. Express **12**, 1485-1496 (2004).

54. R. Thapa, K. Knabe, M. Faheem, A. Naweed, O. L. Weaver, and K. L. Corwin, "Saturated absorption spectroscopy of acetylene gas inside large-core photonic bandgap fiber," Opt. Lett. **31**, 2489-2491 (2006).

55. J. Henningsen, J. Hald, and J. C. Peterson, "Saturated absorption in acetylene and hydrogen cyanide in hollow-core photonic bandgap fibers," Opt. Express **13**, 10475-10482 (2005).

56. C. Wang, N. V. Wheeler, J. K. Lim, K. Knabe, M. D. W. Grogan, Y. Wang, B. R. Washburn, F. Benabid, and K. L. Corwin, "Portable Acetylene Frequency References inside Sealed Hollow-core Kagome Photonic Crystal Fiber," in *Conference on Lasers and Electro-Optics* (Maryland, MD, 2011), p. CFC1.

57. W. C. Swann, and S. L. Gilbert, "Pressure-induced shift and broadening of 1510-1540-nm acetylene wavelength calibration lines," J. Opt. Soc. Am. B **17**, 1263-1270 (2000).

58. C. Wang, S. Wu, B. Mangan, L. Meng, J. M. Fini, R. S. Windeler, E. M. Monberg, A. Desantolo, K. Mukasa, J. W. Nicholson, D. DiGiovanni, B. R. Washburn, and K. L. Corwin, "Single-mode hollow-core fiber for portable acetylene sub-Doppler frequency reference," in *CLEO: 2014*(Optical Society of America, San Jose, California, 2014), p. SM3N.7.

59. F. Benabid, and P. J. Roberts, "Linear and nonlinear optical properties of hollow core photonic crystal fiber," Journal of Modern Optics **58**, 87-124 (2011).

60. K. Kevin, "Using saturated absorption spectroscopy on acetylene-filled Hollow-core fibers for absolute frequency measurements," Ph.D. thesis in *Physics,* (Kansas State University, 2010).

61. J. M. Fini, J. W. Nicholson, R. S. Windeler, E. M. Monberg, L. Meng, B. Mangan, A. DeSantolo, and F. V. DiMarcello, "Low-loss hollow-core fibers with improved single-modedness," Optics Express **21**, 6233-6242 (2013).

Personnel who worked on the project during the grant period: (those in bold are currently working on the project)

Faculty: **Kristan L. Corwin (PI)**
                                  Brian R. Washburn (co-PI)
Post-Docs: none
Graduate Students: **Shun Wu** (05/2008 –05/2014) Ph. D. (direct support)
                                  Chenchen Wang (05/2009 – 05/2015)Ph. D. (direct support)
                                  May Ebini (05/2010 – 12/2011) M. S. (partial direct support)
                                  Tuerghun Maitiniyazi (xx - 08/2014) M.S. (direct support)

                                  Hu Xiaohong (visited until Fall 2013, student from XIOPM, China, fully funded by his home institution)
Xi'an Institute of Optics and Precision Mechanics (XIOPM) of the Chinese Academy of Sciences, in Xi'an, China. XIOPM is one of the largest research institutes in northwest China. It is a comprehensive institute of high-tech innovation and applied fundamental research. The State Key Laboratory of Transient Optics and Photonics (SKLTOP), located in XIOPM, is a leading national research center for transient optics technology and has received numerous scientific awards in China.

Undergraduate Students: **Stephen Meinhardt**, (01/ 2012 –12/2012) B.S.
                                         Mechanical and Nuclear engineering
                                  Mattithya Tillotson, (1/2012 – 05/2014) B. S.
                                         Physics, Chemistry, and Elementary Education
                                  Ryan Luder, (05/2014 – present), pursuing B.S. physics

Publications:
Theses and Reports:

1. Chenchen Wang, Ph.D. thesis, "Optical frequency references in acetylene-filled hollow-core optical fiber and photonic microcells," Kansas State University, 2015.
    https://jrm.phys.ksu.edu/theses.html#Wang-C-PhD

2. Shun Wu, Ph.D. thesis, "Direct fiber laser frequency comb stabilization via single tooth saturated absorption spectroscopy in hollow-core fiber," Kansas State University, 2014.
    https://jrm.phys.ksu.edu/theses.html#Wu-PhD

3. Turghun Matniyaz, M.S. thesis, "Free-space NPR mode locked erbium doped fiber laser based frequency comb for optical frequency measurement," Kansas State University, 2014.
    https://jrm.phys.ksu.edu/theses.html#Matniyaz-MS

4. May Ebini, M.S. report, "Watt-class continuous wave Er^{3+}/Yb^{3+} fiber amplifier", Kansas State University, 2012.
    https://jrm.phys.ksu.edu/theses.html

Peer-Reviewed Publications:
Published in peer-reviewed journals:

1. Shun Wu, Chenchen Wang, Coralie Fourcade-Dutin, Brian R. Washburn, Fetah Benabid, and Kristan L. Corwin, "Direct fiber comb stabilization to a gas-filled hollow-core photonic crystal fiber," Opt. Express 22, 23704-23715 (2014)
http://www.opticsinfobase.org/oe/abstract.cfm?URI=oe-22-19-23704
2. Chenchen Wang, Natalie V. Wheeler, Coralie Fourcade-Dutin, Michael Grogan, Thomas D. Bradley, Brian R. Washburn, Fetah Benabid, and Kristan L. Corwin , "Acetylene frequency references in gas-filled hollow optical fiber and photonic microcells," Applied Optics, Vol. 52, Issue 22, pp. 5430-5439 (2013)
http://www.opticsinfobase.org/ao/abstract.cfm?uri=ao-52-22-5430)

Published in peer-reviewed conference proceedings:
3. C. Wang, S. Wu, B. Mangan, L. Meng, J. M. Fini, R. S. Windeler, E. M. Monberg, A. Desantolo, K. Mukasa, J. W. Nicholson, D. DiGiovanni, B. R. Washburn, and K. L. Corwin, "Single-mode hollow-core fiber for portable acetylene sub-Doppler frequency reference," in CLEO: 2014, OSA Technical Digest (online) (Optical Society of America, 2014), paper SM3N.7.
http://www.opticsinfobase.org/abstract.cfm?URI=CLEO_SI-2014-SM3N.7
4. C. Wang, S. Wu, C. Fourcade Dutin, B. R. Washburn, F. Benabid, and K. L. Corwin, "Toward an all-fiber based optically referenced frequency comb," in CLEO: 2014, OSA Technical Digest (online) (Optical Society of America, 2014), paper SW1O.7.
http://www.opticsinfobase.org/abstract.cfm?URI=CLEO_SI-2014-SW1O.7
5. S. Wu, C. Wang, C. Fourcade Dutin, B. R. Washburn, F. Benabid, and K. L. Corwin, "Direct Comb Stabilization to a $^{12}C_2H_2$-filled Hollow-core Fiber via Single Tooth Saturated Absorption Spectroscopy," in CLEO: 2014, OSA Technical Digest (online) (Optical Society of America, 2014), paper SW1O.1.
http://www.opticsinfobase.org/abstract.cfm?URI=CLEO_SI-2014-SW1O.1
6. S. Wu, C. Wang, C. Fourcade-Dutin, B. R. Washburn, F. Benabid, and K. L. Corwin, "Sub-Doppler Intrafiber Spectroscopy of C2H2 Using Amplified Frequency Comb Lines Directly," in *CLEO: 2013*, OSA Technical Digest (online) (Optical Society of America, 2013), paper CTu3I.1. http://www.opticsinfobase.org/abstract.cfm?URI=CLEO_SI-2013-CTu3I.1
7. Chenchen Wang, Thomas Bradley, Yingying Wang, Kristan L. Corwin, Frédéric Gérôme, and Fetah Benabid, "Angle splice of large-core kagome hollow-core photonic crystal fiber for gas-filled microcells," CLEO: Science and Innovations, San Jose, California United States, June 9-14, 2013, Special Fiber Design & Fabrication (CM3I)
http://www.opticsinfobase.org/abstract.cfm?URI=CLEO_SI-2013-CM3I.1
8. Shun Wu, Chenchen Wang, Coralie Fourcade-Dutin, Brian R. Washburn, Fetah Benabid, and Kristan L. Corwin, "Direct Stabilization of a Frequency Comb to a $^{12}C_2H_2$-filled Hollow-core Photonic Crystal Fiber", Frontiers in Optics, Orlando, FL, October 2013 Frequency Comb Science and Technology I (FTu1A)
http://www.opticsinfobase.org/search.cfm?meetingid=56&year=2013&meetingsession=FTu1A
9. Chenchen Wang, Nathalie V. Wheeler, Coralie F. Dutin, Michael Grogan, Tom Bradley, Brian R. Washburn, Fetah Benabid, and Kristan L. Corwin, "Accurate Fiber-based Acetylene

Frequency References", Conference Paper, CLEO: Science and Innovations, San Jose, California, May 6, 2012, Optical Combs and Spectroscopic Applications (CF2C) http://www.opticsinfobase.org/abstract.cfm?URI=CLEO: S and I-2012-CF2C.7

10. C. Wang, N. V. Wheeler, J. Lim, K. Knabe, M. Grogan, Y. Wang, B. R. Washburn, F. Benabid, and K. L. Corwin, "Portable Acetylene Frequency References inside Sealed Hollow-core Kagome Photonic Crystal Fiber," in *CLEO:2011 - Laser Applications to Photonic Applications*, OSA Technical Digest (CD) (Optical Society of America, 2011), paper CFC1.
http://www.opticsinfobase.org/abstract.cfm?URI=CLEO_SI-2011-CFC1

Interactions/Transitions:
(additional contributed peer-reviewed conference proceedings are listed above)
Invited Talks
 "Counting the frequency of light: Gas-filled hollow optical fibers for novel lasers and frequency metrology" Ball State Physics Colloquium, March 27, 2014
 "Novel lasers and optical frequency references based on gas-filled kagomé fibers," at XLIM/Universite of Limoges, France, hosted by Fetah Benabid , April 11, 2013.
 "Microstructured optical fiber for frequency metrology and optically-pumped gas lasers," Kristan L. Corwin, OSA Traveling lecturer program, presented to meeting of OSA student chapter at the University of New Mexico, March 2, 2012.
 "Acetylene-filled Hollow-core Kagome Fiber toward Portable Frequency References", Kristan L. Corwin, Chenchen Wang, Kevin Knabe, Shun Wu, Jinkang Lim, Brian R. Washburn, Natalie Wheeler, François Couny, and Fetah Benabid, IEEE Photonics Society Annual Meeting,   Denver   CO,   November   11,   2010 http://www.photonicsconferences.org/ANNUAL2010/advancedPrograms.php
 "10 kHz Accuracy Spectroscopy in Acetylene-filled Hollowcore Kagome Fiber and Improved Linewidths", K. L. Corwin, K. Knabe, C. Wang, S. Wu, J. Lim, N. Wheeler, F. Couny, B. R. Washburn, and F. Benabid, Frontiers in Optics Conference (Optical Society of America) , Rochester NY, October 25, 2010

Contributed Talks   (see above under peer-reviewed conference proceedings)

New discoveries, inventions, or patent disclosures:

An invention disclosure was filed internally in June 2015. A provisional patent is anticipated by Fall 2015.

Honors/Awards:
Shun Wu was a finalist for the 2013 Emil Wolf Outstanding Student competition.

Washburn Awards:
Presidential Award for Excellence in Undergraduate Teaching,   2015
        K-State's most prestigious teaching award.
Washburn Service at the national level:
        Conference on Lasers and Electro-Optics Sub-committee member   2012-present
                Topical Group 14: Optical Metrology

Corwin Awards:
    Ad Astra top 150 scientists in Kansas   2011

Corwin Service at the national level:
    Executive Committee Member: APS Division of Laser Sciences   2013 - present
    APS Division of Laser Sciences thesis prize committee member   2014 - present
    National Research Council Committee on Atomic, Molecular and
        Optical Sciences   2012 - 2015

Appendix:
Abstracts of each thesis, in reverse chronological order.
Hyperlinks to each thesis appear above.

OPTICAL FREQUENCY REFERENCES IN ACETYLENE-FILLED HOLLOW-CORE OPTICAL FIBER AND PHOTONIC MICROCELLS

by

CHENCHEN WANG

B.S., University of Science and Technology of China, 2008

AN ABSTRACT OF A DISSERTATION

Submitted in partial fulfillment of the requirements for the degree

DOCTOR OF PHILOSOPHY

Department of Physics
College of Arts and Sciences
KANSAS STATE UNIVERSITY
Manhattan, Kansas
2015

Abstract

Optical frequency references have been widely used in applications such as navigation, remote sensing, and telecommunication industry. For stable frequency references in the near-infrared (NIR), lasers can be locked to narrow absorption features in gases such as acetylene. Currently, most Near NIR references are realized in free space setups. In this thesis, a low-loss hollow-core optical fiber with a diameter of sub millimeters is integrated into the reference setup to provide long interaction lengths between the filling gas and the laser field, also facilitate the optical interaction with low power levels. To make portable NIR reference, gas can be sealed inside the hollow-core fiber, by creating a photonic microcell. This work has demonstrated all-fiber optical frequency references in the Near IR by fabricating and integrating gas sealed photonic microcells in the reference setup. Also, a thoughtful study regarding the lineshape of the fiber-based reference has been accomplished. According the proper modeling of a shift due to lineshape, a correction was applied to our previous absolute frequency measurement of an NIR optical frequency reference. Furthermore, effects of the hollow-core fibers, including mode-dependence frequency shift related to surface modes are explored. In addition, angle splicing techniques, which will improve the performance of the fiber-based frequency reference have been created. Low transmission and return loss angle splices of photonic bandgap fiber, single mode PCF, and large core kagome to SMF-28 are developed and those fibers are demonstrated to be promising for photonic microcell based optical frequency references. Finally, a potentially portable optical metrology system is demonstrated by stabilizing a fiber-laser based frequency comb to an acetylene-filled optical fiber frequency reference. Further work is necessary to fabricate an all-fiber portable optical metrology system with high optical transmission and low molecular contamination.

FREE-SPACE NPR MODE LOCKED ERBRIUM DOPED FIBER LASER BASED FREQUENCY COMB FOR OPTICAL FREQUENCY MEASUREMENT

by

TURGHUN MATNIYAZ

B.Eng., Harbin Institute of Technology, 2011

A THESIS

submitted in partial fulfillment of the requirements for the degree

MASTER OF SCIENCE

Department of Physics

College of Arts and Sciences

KANSAS STATE UNIVERSITY

Manhattan, Kansas

2014

Approved by:

Major Professor

Brian R. Washburn

Abstract

This thesis reports our attempt towards achieving a phase stabilized free-space nonlinear polarization rotation (NPR) mode locked erbium doped fiber laser frequency comb system. Optical frequency combs generated by mode-locked femtosecond fiber lasers are vital tools for ultra-precision frequency metrology and molecular spectroscopy. However, the comb bandwidth and average output power become the two main limiting elements in the application of femtosecond optical frequency combs.

We have specifically investigated the free-space mode locking dynamics of erbium-doped fiber (EDF) mode-locked ultrafast lasers via nonlinear polarization rotation (NPR) in the normal dispersion regime. To do so, we built a passively mode-locked fiber laser based on NPR with a repetition rate of 89 MHz producing an octave-spanning spectrum due to supercontinuum (SC) generation in highly nonlinear fiber (HNLF). Most significantly, we have achieved highly stable self-starting NPR mode-locked femtosecond fiber laser based frequency comb which has been running mode locked for the past one year without any need to redo the mode locking.

By using the free-space NPR comb scheme, we have not only shortened the cavity length, but also have obtained 5 to 10 times higher output power (more than 30 mW at central wavelength of 1570 nm) and much broader spectral comb bandwidth (about 54 nm) compared to conventional all-fiber cavity structure with less than 1 mW average output power and only 10 nm spectral bandwidth. The pulse output from the NPR comb is amplified through a 1 m long EDF, then compressed by a length of anomalous dispersion fiber to a near transform limited pulse duration. The amplified transform limited pulse, with an average power of 180 mW and pulse duration of 70 fs, is used to generate a supercontinuum of 140 mW. SC generation via propagation in HNLF is optimized for specific polling period and heating temperature of PPLN crystal for SHG around 1030 nm. At last, we will also discuss the attempt of second harmonic generation (SHG) by quasi phase matching in the periodically polled lithium niobate (PPLN) crystal due to nonlinear effects corresponding to different polling period and heating temperature.

DIRECT FIBER LASER FREQUENCY COMB STABILIZATION VIA SINGLE TOOTH SATURATED ABSORPTION SPECTROSCOPY IN HOLLOW-CORE FIBER

by

SHUN WU

B.S., Beijing Normal University, 2005
M.S., Michigan Technological University, 2007
AN ABSTRACT OF A DISSERTATION

submitted in partial fulfillment of the requirements for the degree

DOCTOR OF PHILOSOPHY

Department of Physics
College of Arts and Sciences

KANSAS STATE UNIVERSITY
Manhattan, Kansas

2014

Abstract

Portable frequency references are crucial for many practical on-site applications, for example, the Global Position System (GPS) navigation, optical communications, and remote sensing. Fiber laser optical frequency combs are a strong candidate for portable reference systems. However, the conventional way of locking the comb repetition rate, f_{rep}, to an RF reference leads to large multiplied RF instabilities in the optical frequency domain. By stabilizing a comb directly to an optical reference, the comb stability can potentially be enhanced by four orders of magnitude. The main goal of this thesis is to develop techniques for directly referencing optical frequency combs to optical references toward an all-fiber geometry.

A big challenge for direct fiber comb spectroscopy is the low comb power. With an 89 MHz fiber ring laser, we are able to optically amplify a single comb tooth from nW to mW (by a factor of 10^6) by building multiple filtering and amplification stages, while preserving the comb signal-to-noise ratio. This amplified comb tooth is directly stabilized to an optical transition of acetylene at 1539.4 nm via a saturated absorption technique, while the carrier-envelope offset frequency, f_0, is locked to an RF reference.

The comb stability is studied by comparing to a single wavelength (or CW) reference at 1532.8 nm. Our result shows a short term instability of 6×10^{-12} at 100 ms gate time, which is over an order of magnitude better than that of a GPS-disciplined Rb clock. This implies that our optically-referenced comb is a suitable candidate for a high precision portable reference. In addition, the direct comb spectroscopy technique we have developed opens many new possibilities in precision spectroscopy for low power, low repetition rate fiber lasers.

For single tooth isolation, a novel cross-VIPA (cross-virtually imaged phase array) spectrometer is proposed, with a high spectral resolution of 730 MHz based on our simulations. In addition, the noise dynamics for a free space Cr:forsterite-laser-based frequency comb are explored, to explain the significant f_0 linewidth narrowing with knife insertion into the intracavity beam. A theoretical model is used to interpret this f_0 narrowing phenomenon, but some unanswered questions still remain.

WATT-CLASS CONTINUOUS WAVE Er3+/Yb3+ FIBER AMPLIFIER

by

MAY EBBENI

B.A., Yarmouk University, 2006

A REPORT

submitted in partial fulfillment of the requirements for the degree

MASTER OF SCIENCE

Department of Physics

College of Arts and Sciences

KANSAS STATE UNIVERSITY

Manhattan, Kansas

2012

Approved by:

Major Professor

Brian R. Washburn

Abstract

Rare-earth doped optical fibers can be used to make optical amplifiers in the near infrared with large optical gain in an all fiber based system. Indeed, erbium doped fibers made gain possible within the 1532 to 1560 nm band which makes long span fiber optical communication systems a possibility. Erbium doped fibers have also been used to make narrow linewidth or mode-locked lasers. Other rare-earth doped fibers can be used for amplifiers in other near-infrared spectral regions. Recently, fiber amplifier technology has been pushed to produce watt level outputs for high power applications such as laser machining. These high power amplifiers make new experiments in ultrafast fiber optics a possibility.

This report reviews the current literature on Watt-class continuous wave erbium doped amplifiers and discussed our attempt to develop a high power Yb/Er amplifier. After the design of the cladding pump in 1999, the world's first single mode fiber laser with a power greater than 100 Watts of the continuous wave light was introduced. After 2002 there was a huge spike in the output powers (up to 2 kW) of lasers based on rare-earth doped fibers. Our own work involved developing a 10 W amplifier at 1532 nm and 1560 nm. A high power amplifier was made by seeding a dual-clad Yb/Er co-doped fiber pumped at 925 nm using a lower power erbium doped fiber amplifier. We will discuss the design and construction of the amplifier, including the technical difficulties for making such an amplifier.

1.

1. Report Type

Final Report

Primary Contact E-mail
Contact email if there is a problem with the report.

corwin@phys.ksu.edu

Primary Contact Phone Number
Contact phone number if there is a problem with the report

785-537-1369

Organization / Institution name

Kansas State University

Grant/Contract Title
The full title of the funded effort.

Direct Spectroscopy In Hollow Optical Fiber With Fiber-Based Optical
Frequency Combs

Grant/Contract Number
AFOSR assigned control number. It must begin with "FA9550" or "F49620" or "FA2386".

FA9550-11-1-0096

Principal Investigator Name
The full name of the principal investigator on the grant or contract.

Kristan L. Corwin

Program Manager
The AFOSR Program Manager currently assigned to the award

Dr. Enrique Parra

Reporting Period Start Date

06/01/2011

Reporting Period End Date

05/31/2015

Abstract

Toward the creation of robust, portable frequency references in the near IR, we have isolated a single tooth
from a fiber laser-based optical frequency comb for nonlinear spectroscopy and thereby directly referenced
the comb. An 89 MHz erbium fiber laser frequency comb is directly stabilized to the P(23) (1539.43 nm)
overtone transition of $12C2H2$ inside a hollow-core photonic crystal fiber. To do this, a single comb tooth is
isolated and amplified from 20 nW to 40 mW with sufficient fidelity to perform saturated absorption
spectroscopy. The fractional stability of the comb, ~ 7 nm away from the stabilized tooth, is shown to be
$6\times10\text{-}12$ at 100 ms gate time, which is over an order of magnitude better than that of a comb referenced to
a GPS-disciplined Rb oscillator.
Furthermore, gas-filled hollow optical fiber references based on the P(13) transition of the $\nu1 + \nu3$ band of
$12C2H2$ promise portability with moderate accuracy and stability. Previous realizations are corrected (<
1σ) using proper modeling of a shift due to line-shape. To improve portability, a sealed photonic microcell
(PMC) is characterized on the $12C2H2$ $\nu1 + \nu3$ P(23) transition with somewhat reduced accuracy and
stability. Effects of the photonic crystal fiber, including surface modes, are explored. Both polarization-
maintaining (PM) and non-PM 7-cell photonic bandgap fiber are shown to be unsuitable for kHz level
frequency references.

Toward improving the portability of the system, Perturbed Resonance for Improved Single Modedness (PRISM) fiber is employed for saturated absorption spectroscopy in a molecular gas. Reduced alignment sensitivity, lack of surface modes, and ease of angle splicing make it promising for portable gas-filled frequency references.

Distribution Statement

This is block 12 on the SF298 form.

Distribution A - Approved for Public Release

Explanation for Distribution Statement

If this is not approved for public release, please provide a short explanation. E.g., contains proprietary information.

SF298 Form

Please attach your SF298 form. A blank SF298 can be found here. Please do not password protect or secure the PDF The maximum file size for an SF298 is 50MB.

June 2015 Corwin Parra.pdf

Upload the Report Document. File must be a PDF. Please do not password protect or secure the PDF . The maximum file size for the Report Document is 50MB.

Final Report 2015 v2.pdf

Upload a Report Document, if any. The maximum file size for the Report Document is 50MB.

Archival Publications (published) during reporting period:

Published in peer-reviewed journals:

1. Shun Wu, Chenchen Wang, Coralie Fourcade-Dutin, Brian R. Washburn, Fetah Benabid, and Kristan L. Corwin, "Direct fiber comb stabilization to a gas-filled hollow-core photonic crystal fiber," Opt. Express 22, 23704-23715 (2014)
http://www.opticsinfobase.org/oe/abstract.cfm?URI=oe-22-19-23704
2. Chenchen Wang, Natalie V. Wheeler, Coralie Fourcade-Dutin, Michael Grogan, Thomas D. Bradley, Brian R. Washburn, Fetah Benabid, and Kristan L. Corwin , "Acetylene frequency references in gas-filled hollow optical fiber and photonic microcells," Applied Optics, Vol. 52, Issue 22, pp. 5430-5439 (2013)
http://www.opticsinfobase.org/ao/abstract.cfm?uri=ao-52-22-5430)

Published in peer-reviewed conference proceedings:
3. C. Wang, S. Wu, B. Mangan, L. Meng, J. M. Fini, R. S. Windeler, E. M. Monberg, A. Desantolo, K. Mukasa, J. W. Nicholson, D. DiGiovanni, B. R. Washburn, and K. L. Corwin, "Single-mode hollow-core fiber for portable acetylene sub-Doppler frequency reference," in CLEO: 2014, OSA Technical Digest (online) (Optical Society of America, 2014), paper SM3N.7.
http://www.opticsinfobase.org/abstract.cfm?URI=CLEO_SI-2014-SM3N.7
4. C. Wang, S. Wu, C. Fourcade Dutin, B. R. Washburn, F. Benabid, and K. L. Corwin, "Toward an all-fiber based optically referenced frequency comb," in CLEO: 2014, OSA Technical Digest (online) (Optical Society of America, 2014), paper SW1O.7.
http://www.opticsinfobase.org/abstract.cfm?URI=CLEO_SI-2014-SW1O.7
5. S. Wu, C. Wang, C. Fourcade Dutin, B. R. Washburn, F. Benabid, and K. L. Corwin, "Direct Comb Stabilization to a 12C2H2-filled Hollow-core Fiber via Single Tooth Saturated Absorption Spectroscopy," in CLEO: 2014, OSA Technical Digest (online) (Optical Society of America, 2014), paper SW1O.1.
http://www.opticsinfobase.org/abstract.cfm?URI=CLEO_SI-2014-SW1O.1
6. S. Wu, C. Wang, C. Fourcade-Dutin, B. R. Washburn, F. Benabid, and K. L. Corwin, "Sub-Doppler Intrafiber Spectroscopy of C2H2 Using Amplified Frequency Comb Lines Directly," in CLEO: 2013, OSA Technical Digest (online) (Optical Society of America, 2013), paper CTu3I.1.
http://www.opticsinfobase.org/abstract.cfm?URI=CLEO_SI-2013-CTu3I.1
7. Chenchen Wang, Thomas Bradley, Yingying Wang, Kristan L. Corwin, Frédéric Gérôme, and Fetah Benabid, "Angle splice of large-core kagome hollow-core photonic crystal fiber for gas-filled microcells," CLEO: Science and Innovations, San Jose, California United States, June 9-14, 2013, Special Fiber

Design & Fabrication (CM3I)
http://www.opticsinfobase.org/abstract.cfm?URI=CLEO_SI-2013-CM3I.1

8. Shun Wu, Chenchen Wang, Coralie Fourcade-Dutin, Brian R. Washburn, Fetah Benabid, and Kristan L. Corwin, "Direct Stabilization of a Frequency Comb to a 12C2H2-filled Hollow-core Photonic Crystal Fiber", Frontiers in Optics, Orlando, FL, October 2013 Frequency Comb Science and Technology I (FTu1A) http://www.opticsinfobase.org/search.cfm?meetingid=56&year=2013&meetingsession=FTu1A

9. Chenchen Wang, Nathalie V. Wheeler, Coralie F. Dutin, Michael Grogan, Tom Bradley, Brian R. Washburn, Fetah Benabid, and Kristan L. Corwin, "Accurate Fiber-based Acetylene Frequency References", Conference Paper, CLEO: Science and Innovations, San Jose, California, May 6, 2012, Optical Combs and Spectroscopic Applications (CF2C) http://www.opticsinfobase.org/abstract.cfm?URI=CLEO: S and I-2012-CF2C.7

10. C. Wang, N. V. Wheeler, J. Lim, K. Knabe, M. Grogan, Y. Wang, B. R. Washburn, F. Benabid, and K. L. Corwin, "Portable Acetylene Frequency References inside Sealed Hollow-core Kagome Photonic Crystal Fiber," in CLEO:2011 - Laser Applications to Photonic Applications, OSA Technical Digest (CD) (Optical Society of America, 2011), paper CFC1.
http://www.opticsinfobase.org/abstract.cfm?URI=CLEO_SI-2011-CFC1

Changes in research objectives (if any):

Change in AFOSR Program Manager, if any:

The program manager changed from Dr. Tatjana Curcic to Dr. Riq Parra during the grant period.

Extensions granted or milestones slipped, if any:

No-cost extension granted.

AFOSR LRIR Number

LRIR Title

Reporting Period

Laboratory Task Manager

Program Officer

Research Objectives

Technical Summary

Funding Summary by Cost Category (by FY, $K)

	Starting FY	FY+1	FY+2
Salary			
Equipment/Facilities			
Supplies			
Total			

Report Document

Report Document - Text Analysis

Report Document - Text Analysis

Appendix Documents

2. Thank You

E-mail user

Jul 06, 2015 15:36:03 Success: Email Sent to: corwin@phys.ksu.edu